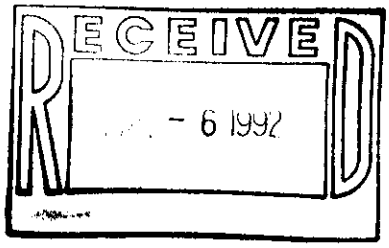

APPLICATION OF A CANINE ^{238}Pu DOSIMETRY MODEL TO HUMAN BIOASSAY DATA

By

ALBERT W. HICKMAN, JR.

DISCLAIMER

A THESIS PRESENTED TO THE GRADUATE SCHOOL
OF THE UNIVERSITY OF FLORIDA IN PARTIAL FULFILLMENT
OF THE REQUIREMENTS FOR THE DEGREE OF
MASTER OF SCIENCE

UNIVERSITY OF FLORIDA

AUGUST 1991

ACKNOWLEDGEMENTS

I would like to thank Dr. Genevieve S. Roessler, committee chair, University of Florida, for her guidance and encouragement, in both the production of this thesis and my graduate studies in general. It was through her influence that I was introduced to health physics and decided to undertake this endeavor.

I would like to thank Dr. Raymond A. Guilmette, committee member, Lovelace Inhalation Toxicology Research Institute, for his help in understanding the biological aspects of biokinetic modeling and for the hospitality extended to me while I was in Albuquerque.

I would like to thank Dr. David E. Hintenlang, committee member, University of Florida, for his willingness to listen and for supplying kicks in the pants when needed.

I would like especially to thank Mr. William C. Griffith, Inhalation Toxicology Research Institute, for his assistance with the mathematical aspects of biokinetic modeling and in the preparation of the figures used in this thesis. His help has been invaluable and is greatly appreciated.

I would like to thank Dr. Lih-Jenn Shyr, Inhalation Toxicology Research Institute, for his help in using the

SimuSolv simulation package on which the modeling work was done.

I would like to thank the other members of the Biomathematics Group at the Inhalation Toxicology Research Institute, including Dr. Joseph H. Diel, one of the developers of the canine model on which this work was based, Ms. I-Yiin Chang, and Dr. Bobby Scott, for their help and encouragement.

I would like to thank my friends at the First Baptist Church of Gainesville and at Sandia Baptist Church in Albuquerque for their support during this process and for helping me to keep the big picture in view. To God be the glory, for without His working in my life the production of this thesis would not have been possible.

I would like to thank my parents for their love and their belief in me during this time, for loving someone and believing in him have great power.

Finally, I would like to thank Oak Ridge Associated Universities for providing funding for my graduate studies. This research was performed under appointment to the Nuclear Engineering and Health Physics Fellowship Program administered by Oak Ridge Associated Universities for the United States Department of Energy (U.S. DOE) and was partially supported by the U.S. DOE under Contract Number DE-AC05-76OR00033.

TABLE OF CONTENTS

LIST OF TABLES

LIST OF FIGURES

Abstract of Thesis Presented to the Graduate School
of the University of Florida in Partial Fulfillment of the
Requirements for the Degree of Master of Science

APPLICATION OF A CANINE ^{238}Pu DOSIMETRY MODEL
TO HUMAN BIOASSAY DATA

By

Albert W. Hickman, Jr.

August 1991

Chairperson: Genevieve S. Roessler, Ph.D.
Major Department: Nuclear Engineering Sciences

Associated with the use of ^{238}Pu in thermoelectric power sources for space probes and power supplies for cardiac devices is the potential for human exposure to ^{238}Pu, primarily by inhalation. In the event of human internal exposure, a means is needed for assessing the level of intake and calculating radiation doses.

Several bioassay/dosimetry models have been developed for ^{239}Pu. However, results from studies with laboratory animals have indicated that the biokinetics, and therefore the descriptive models, of ^{238}Pu are significantly different from those for ^{239}Pu. A canine model accounting for these differences (J.A. Mewhinney and J.H. Diel, Health Physics 45, 39-60 [1983]) has been applied in this work to urinary excretion data from seven humans occupationally exposed to low levels of an insoluble ^{238}Pu compound. The modified model

provides a good description of the urinary excretion kinetics observed in the exposed humans. The modified model was also used to provide estimates of the initial intakes of ^{238}Pu for the seven individuals; these estimates ranged from 4.5 nCi (170 Bq) to 87 nCi (3200 Bq). Autopsy data on the amount and distribution of ^{238}Pu retained in the organs may be used in the future to validate or refute both these estimates and the assumptions used to formulate the human model. Modification of the human model to simulate an injection exposure to ^{239}Pu gave patterns of retention in the organs and urinary excretion comparable to those seen previously in humans; further modification of the model using fecal data (unavailable for the subjects of this study) is indicated.

CHAPTER 1
OBJECTIVES OF RESEARCH

Plutonium-238 has a half-life of 87.7 y (Walker et al., 1989) and decays by emitting a 5.4 MeV α particle with relatively little associated γ radiation (Stannard, 1973). These characteristics make this radionuclide useful as a heat source in specialized situations, including thermoelectric generators used in space probes and power supplies for cardiac pacemakers (Stannard, 1973). Potential applications include the use of ^{238}Pu to power artificial hearts and as a pure heat source in some medical applications. Thus, the potential exists for accidental exposure of workers or the general public to Pu, potentially as $^{238}PuO_2$.

The principal exposure pathway of concern is inhalation. For example, in the "Final Safety Analysis Report for the Ulysses Mission" (US DOE, 1990), direct inhalation following a launch-pad or near-launch-pad accident is cited as the primary focus for mission risk assessment, because it involves the highest doses to individuals. Exposure via this pathway may be unavoidable unless people living in the projected pathway of the cloud are evacuated. Inhalation of material deposited on the ground is of somewhat lesser importance. Ingestion of contaminated food or water is considered less

important, relative to direct inhalation, because Pu is not readily absorbed through the gastrointestinal tract (ICRP, 1986).

In the event of an inhalation exposure, a means for assessing the amount of Pu deposited in the lung is necessary for planning medical treatment, if needed, and predicting the dose which will result from the exposure. One method of estimating the activity deposited in the body following an exposure is through the use of mathematical models applied to measurements of activity in excreta. Models developed for use following exposure to Pu include those of Langham et al. (1950), Beach and Dolphin (1964), Durbin (1972), the International Commission on Radiological Protection (ICRP, 1987), and Leggett and Eckerman (1987). Those models which might be used following an inhalation exposure were developed using data on exposure to ^{239}Pu.

Biologic effects observed in beagles following inhalation exposures to $^{238}PuO_2$ are different than those seen following exposure to $^{239}PuO_2$ at similar levels of radioactivity initially deposited in the lung (initial lung burden, or ILB) (Muggenburg et al., 1980; Park et al., 1980). Plutonium inhaled as $^{238}PuO_2$ is cleared more rapidly from the lung to the systemic circulation, and from there to the liver and skeleton, than is Pu inhaled as $^{239}PuO_2$. This increased clearance has been attributed to a specific-activity-dependent breakup of the $^{238}PuO_2$ particles. The exact mechanisms have

not been described, but Fleischer and Raabe (1977) have postulated that the recoil nuclei resulting from α decay cause the ejection of fragments of PuO_2 from the particle. Turcotte (1976) has observed radiation damage resulting primarily from the recoil nuclei in macroscopic powders of actinide dioxides, but the generalizability of this phenomenon to sub-micron sized particles is uncertain.

Diel and Mewhinney utilized lung retention data from beagles exposed to monodisperse aerosols of $^{238}PuO_2$ (aerosols with a narrow size distribution, i.e. geometric standard deviation ≤ 1.2) and data from lung autoradiographs from these same dogs (Diel and Mewhinney, 1983) to develop a model (Mewhinney and Diel, 1983) describing the behavior of inhaled $^{238}PuO_2$. They had previously noted (Diel and Mewhinney, 1980) that the differences in the behavior of inhaled $^{238}PuO_2$ and $^{239}PuO_2$ have several important implications for assessing the hazards following an inhalation exposure to $^{238}PuO_2$. First, data must be obtained over a long period of time (for at least two years following inhalation) in order to accurately assess the radiation dose to lung, liver, and skeleton. Second, urinary excretion of ^{238}Pu increases with time following inhalation exposure, and this must be considered when using urinary excretion data to assess the amount of material present in the lungs following such an exposure. Third, because of the differences in translocation of Pu isotopes and the increased dispersion of ^{238}Pu in lung tissue, relative to

^{239}Pu, parameters derived from $^{239}PuO_2$ studies or exposure incidents should not be used to evaluate $^{238}PuO_2$ incidents. Finally, the organs at risk following inhalation seem to be different for $^{238}PuO_2$ and $^{239}PuO_2$. They further noted that the phenomena observed in beagles probably would occur in humans as well (Diel and Mewhinney, 1981).

Linkages established between the Inhalation Toxicology Research Institute (ITRI) and internal dosimetry professionals at a United States Department of Energy laboratory have resulted in the availability for further study of urinary excretion data from seven humans occupationally exposed via inhalation to low levels of ^{238}Pu (personal communication, J.N.P. Lawrence to R.A. Guilmette). The uniqueness of these data in terms of both the length of time during which samples were collected and analyzed and the low level of detection of Pu in urine for the radiochemistry techniques used make possible the data's use in this study in developing a metabolic model to describe the behavior of inhaled ^{238}Pu in humans and the use of that model to estimate the initial lung burdens (ILBs) received by the exposed individuals. External measurements of inhaled activity have proved unusable for these individuals because the workers had previous low-level occupational exposure to ^{137}Cs. Although the radiation dose delivered by this exposure is negligible, the levels of ^{137}Cs activity present are sufficient to render external counting techniques ineffective in this situation. Therefore, analysis

of excreta is necessary in order to determine the workers' ILBs.

Applying existing models of the behavior of inhaled Pu to these data further illustrate the need for a separate model for use following inhalation of ^{238}Pu compounds. Table 1-1 contains the results of using the model developed by the International Commission on Radiological Protection (ICRP, 1987) to estimate ILB for one of the exposed individuals, assuming exposure to particles 1 μm in diameter. While the estimates should remain consistent over the entire time range observed, they vary from 1 nCi (40 Bq) at 3 d post exposure to 5500 nCi (200 kBq) at 5070 d post-exposure, an increase of over three orders of magnitude.

TABLE 1-1

Variation in Initial Lung Burden Estimated Using the ICRP (1987) Method with Measurements of Activity in Urine

Time After Exposure	Fraction Inhaled Activity Excreted	Activity in Urine		Estimated Initial Lung Burden	
days	(ICRP)	pCi	mBq	nCi	kBq
3	8.5×10^{-6}	0.01	0.4	1	4×10^{-2}
30	9.5×10^{-7}	0.15	5.6	160	5.8
94	7.0×10^{-7}	0.78	29	1100	4.1×10^{1}
499	7.5×10^{-7}	2.84	105	3800	1.4×10^{2}
999	8.0×10^{-7}	2.25	83.3	2800	1.0×10^{2}
5070	3.2×10^{-7}	1.75	64.8	5500	2.0×10^{2}

Thus, the availability of a canine model that reasonably described the biokinetics of inhaled $^{238}PuO_2$, the completeness and uniqueness of the human data from an inhalation exposure to ^{238}Pu, the deficiencies of current models used to describe the excretion of this material, and the need for accurate models in the event future exposures occur combine to make the development of a ^{238}Pu biokinetic model and its application to the existing data both feasible and practical. Therefore, this study contributes to the science of ^{238}Pu dosimetry by the development of a human metabolic model of inhaled ^{238}Pu. Chapter 2 of this thesis describes the background to the development of the human model, including the principles of both bioassay and mathematical modeling and a description of the canine model used in this study. The methodology used in adapting the canine model for use with human data is described in Chapter 3. Chapter 4 presents the results of the adaptation process, along with conclusions to be drawn from the study and recommendations for future work. SimuSolv (Dow Chemical Company, Midland, MI) modeling and simulation software was used to modify the canine model for use with humans and to estimate the initial lung burdens received by the exposed individuals. An appendix contains the code for the final version of the model.

CHAPTER 2
BACKGROUND TO RESEARCH

Definition of Bioassay

Bioassay is the determination, either by direct measurement (in-vivo assessment) or by analysis of material excreted or removed from the body (in-vitro assessment), of the kind, amount, location, and/or retention of radionuclides in the body. Radiation protection programs often include the use of bioassay techniques to monitor workers for internal exposure to radioactive materials and to assess the need for radiation protection measures in addition to those currently provided. Such methods also can be used to determine whether and what kinds of medical intervention are needed in cases of accidental exposures.

Bioassay Techniques

In-Vivo Methods

In-vivo methods are used to estimate directly the amount of a radionuclide/radionuclides (body burden) in a living subject (NCRP, 1987), by either whole-body or partial-body counting. They are feasible only for those radionuclides that emit radiation which can escape from the body (ICRP, 1987).

Such emitted radiations include X and γ rays; positrons (which can be detected by measurement of annihilation radiation); energetic β particles (detected by measuring bremsstrahlung); and some characteristic X rays which follow α decay. In-vivo techniques are, in general, not useful in detecting those radionuclides that emit α particles accompanied only by weak characteristic X rays.

Many devices used to measure activity in the body utilize solid inorganic scintillators such as thallium-activated sodium iodide (NaI[Tl]) detectors (NCRP, 1987). Very simple instruments without energy-discrimination capabilities can be used to assess the total activity in the body if the radionuclide of concern is known. More complex facilities are needed to determine distribution patterns within the body and to give specific information on the radionuclide or radionuclides taken into the body, if those are unknown.

In-vivo counting done as part of routine radiation protection activities usually is conducted within a room shielded from background radiation with steel or lead. The subject sits in a chair or lies on a reclining chair or other curved surface. In the simplest systems, a single detector is placed a short distance from the subject. In more complex systems, multiple fixed-position detectors are used to provide increased sensitivity and geometric independence (e.g. using separate detectors for the thyroid, lungs, and gastrointestinal tract). An alternative system utilizes a

single crystal or array of crystals which moves along the length of the subject's body or under which the subject is moved. Such a system gives both total activity present in the body and a profile of the distribution of the radioactive material within the body.

Detectors using solid or liquid organic scintillators can be used to determine body burden as well. Such detectors are usually hollow cylinders, with the subject placed in the middle, along the centerline. Because of their geometry, these detectors have high counting efficiency and relatively high sensitivity for detecting whole-body activity. However, they have poor energy resolution and provide no information on the distribution of radionuclides within the body.

Germanium, Si, and gas-filled proportional counters have been used in whole-body counting. High-efficiency Ge detectors in combination with multichannel analyzers are especially useful in determining the composition of mixtures of γ-ray emitting radionuclides. High-purity Ge detectors have been used to quantitate lung burdens of α emitters with low-energy associated X rays, such as ^{238}Pu.

Assessment of activity in wounds is fairly simple for γ emitters, requiring only a conventional β-γ detector. As with other types of exposures, detection of α emitters is difficult, especially when the contamination is deep within the wound, and estimating activity for each component of a

mixture requires the use of detectors with good energy discrimination capabilities.

Use of a phoswich in-vivo counting system was attempted with the subjects of this study (personal communication, Rick Brake). This system observes the γ spectrum between 17 and 100 keV, dividing it into three regions of interest: 17 keV (Region 1), 60 keV (Region 2), and 80-100 keV (Region 3). Plutonium-238 emits characteristic X rays of energy 13.5-20 keV, with the most abundant and nominal average energy being 17 keV. The 80-100 keV region is used as a reference region for correcting for background radiation (for example, ^{40}K present in the body produces Compton photons with energies falling in both the 17 keV and 80-100 keV ranges). The net counts observed in the 17-keV region are calculated by

$$N_1 = G_1 - B_1 - K_1(G_3 - B_3) \qquad (1)$$

where N_1 = Net counts in region 1,

G_i = Gross counts in region i,

B_i = Background counts in region i without the subject (a source of both ^{40}K and scatter) present, and

K_1 = (Average counts in region 1)/ (Average counts in region 3) for a radioactively "clean" person.

K_1 is a constant, because larger persons have more ^{40}K in their bodies but also more scatter from their larger mass. N_1 depends on K_1 and further depends on the 1.46 MeV ^{40}K γ rays dominating the Compton photon production.

The presence of a radionuclide which emits γ rays of lower energy changes the shape of the emission spectrum. This destroys the ability to obtain a valid K_1 and thus a valid N_1. For example, the presence of 0.5 nCi (18.5 Bq) ^{137}Cs in an individual (which would be difficult to detect as an explicit peak in the photon emission spectrum) will cause a negligible radiation dose to the person but will cause an increase in the number of photons produced with energies 80-100 keV (because of Compton interactions). K_1 then becomes a function of levels of Cs which cannot be quantitated, and values of N_1 (net counts in the ^{238}Pu γ-emission spectrum) cannot be determined. Because the individuals in this study exposed to $^{238}PuO_2$ had received previous low-level work-related exposure to ^{137}Cs which could not be quantitated, in-vivo counting methods were of little use in determining initial lung burdens of ^{238}Pu, although the levels of ^{238}Pu were suspected to be such that they would have been detectable in the absence of the ^{137}Cs.

In-Vitro Methods

Tissue samples (including biopsy specimens) can be analyzed using radiochemical techniques to give a direct estimate of an individual's intake (the quantity of radioactive material entering the body, primarily via inhalation, ingestion, or through a wound or intact skin) and

uptake (the quantity of radioactive material transferred from the site of intake to body organs and/or tissues) of a radionuclide (Boecker et al., 1991). However, such analyses rarely are performed on living persons (NCRP, 1987). Instead, various other samples are analyzed, including urine, feces, blood, sweat, breath, hair, fingernails, saliva, and teeth (Boecker et al., 1991). The results of these analyses, unfortunately, provide only an indirect measure of the internal deposition of a radionuclide. Metabolic models, which allow estimates of organ burdens to be made based on these in-vitro measurements by quantifying the relationship between the two, will be discussed in the next section.

Urine analysis

Urine analysis is the most commonly used in-vitro bioassay technique today. It is most easily applied for radionuclides that enter the body in relatively soluble form and for radionuclides that distribute uniformly throughout the whole body (such as ^{3}H and ^{137}Cs). Material internally deposited within the body that is cleared to the blood is in turn transferred to the organs or excreted, primarily via the urine. Material in the organs is recirculated back to the blood at varying rates, from which it is recycled back to the organs or excreted in the urine and feces.

In most cases, urine samples represent a collection over a 24-h period or its equivalent. The samples are chemically treated to separate out the radionuclide(s) of interest, and

the amount of activity present is assessed. For routine radiation protection purposes, this analysis is used to identify individuals with excretion greater than the expected background amounts. In the presence of such elevated levels, or after a known accidental exposure, successive samples are analyzed to obtain levels and patterns of excretion of radioactivity so that intake can be determined.

Fecal analysis

Analysis of feces is less common than urine analysis, although it can provide useful information that urine analysis cannot, especially about exposures to insoluble compounds. After an ingestion exposure, the feces will contain the fraction of radioactive material not absorbed into the bloodstream. The radionuclides that enter the blood will be transferred to the organs, with some portion of the transferred material taken up by the liver excreted in the feces by way of the bile.

After an inhalation exposure, inhaled material that deposits in the nasal passages, trachea, and bronchi will be cleared mechanically via mucociliary action to the pharynx, where it is swallowed and enters the gastrointestinal tract. If the inhaled material is highly soluble in extracellular fluid, some of the material may be absorbed directly into the blood as well. Swallowed material that is not absorbed into the bloodstream in the gastrointestinal tract is excreted in the feces. Material that is deposited in the pulmonary region

of the lungs is absorbed into the bloodstream at a rate depending upon its solubility. Soluble material is rapidly absorbed; insoluble material may be retained in the pulmonary region for a period of years. Radionuclides appearing in the feces during this time have been cleared mechanically through the nasopharyngeal and tracheobronchial regions of the lung and swallowed or are being excreted into the feces from the liver, via the bile.

Use of fecal analysis does present several problems. Since material can enter the feces by several different pathways, a good knowledge of the clearance mechanisms at work in the situation under study is essential. In addition, collection and analysis of samples are more difficult. Fecal excretion exhibits a greater variability between individuals, and even within the same individual from day to day, than does urinary excretion. In the United States, fecal samples are more difficult to obtain than are urine samples (and they were not available for the subjects of this study), although this appears to be less so in Europe. Nonetheless, analysis of fecal excretion can give significant information.

Analysis of other biologic material

Other samples may be analyzed for radionuclide content as aids in determining intake and uptake, but these are less common. As mentioned previously, analyses of tissues from living persons are unusual. By themselves, such analyses can confirm that an uptake has occurred, but they give no

information on the time or amount of the exposure. Breath samples can be analyzed for radionuclides present in the gas or vapor phase, such as ^{222}Rn (a decay product of ^{226}Ra), ^{220}Rn (a decay product of ^{228}Th and ^{232}Th), ^{14}C in $^{14}CO_2$, and ^{3}H in HTO.

Blood samples are available only in small amounts, and although they may show less fluctuation in activity levels than do urine samples, they are of limited use when the radionuclide of interest is rapidly taken up from the blood by the organs and only slowly re-released to the blood. However, blood samples may be useful in cases of exposure to high levels of a radioactive material. Analysis of other biologic materials, such as hair, sweat, and teeth, finds only limited use in specialized circumstances.

Use of any biologic material for bioassay, including urine and feces, is not without potential problems. Excretion patterns vary both among individuals and from day to day for a given individual. Analysts also must control for differences in length of sampling period, if they exist. In addition, care must be taken to avoid contamination of the sample with foreign radioactive material and to minimize losses of material from the sample during analysis.

Mathematical Models

Mathematical models enable radiation protection personnel to interpret measurements of activity in the whole body or in excreta in terms of intake or dose. Also called "metabolic

models," they provide a mathematical description of intake, uptake, distribution, retention, and excretion. These models are developed using knowledge and assumptions about both the biological and physical/chemical behavior, in the whole body and in specific organs, of the radioactive materials of interest.

Metabolic models represent the body as a series of compartments into and out of which the radioactive material moves at various rates, with removal from the body occurring by excretion, radioactive decay, or both. The mathematical relationships between radionuclide intake, uptake, and excretion allow the estimation of intake and uptake based on excretion measurements. Estimates of dose from a given intake and/or uptake are made using the relationships between the latter two quantities, distribution, and retention and the radioactive decay characteristics of the radionuclide of interest.

Routes of intake of radioactive material into the body are depicted as large arrows in Figure 2-1. Representative compartments (organs and tissues) are depicted as boxes, with potential excretion routes useful for bioassay measurement depicted as circles. The intake routes (mentioned previously) and their general features are listed below.

1. Inhalation. Airborne radioactive material may be taken into the respiratory tract, which can be divided into three

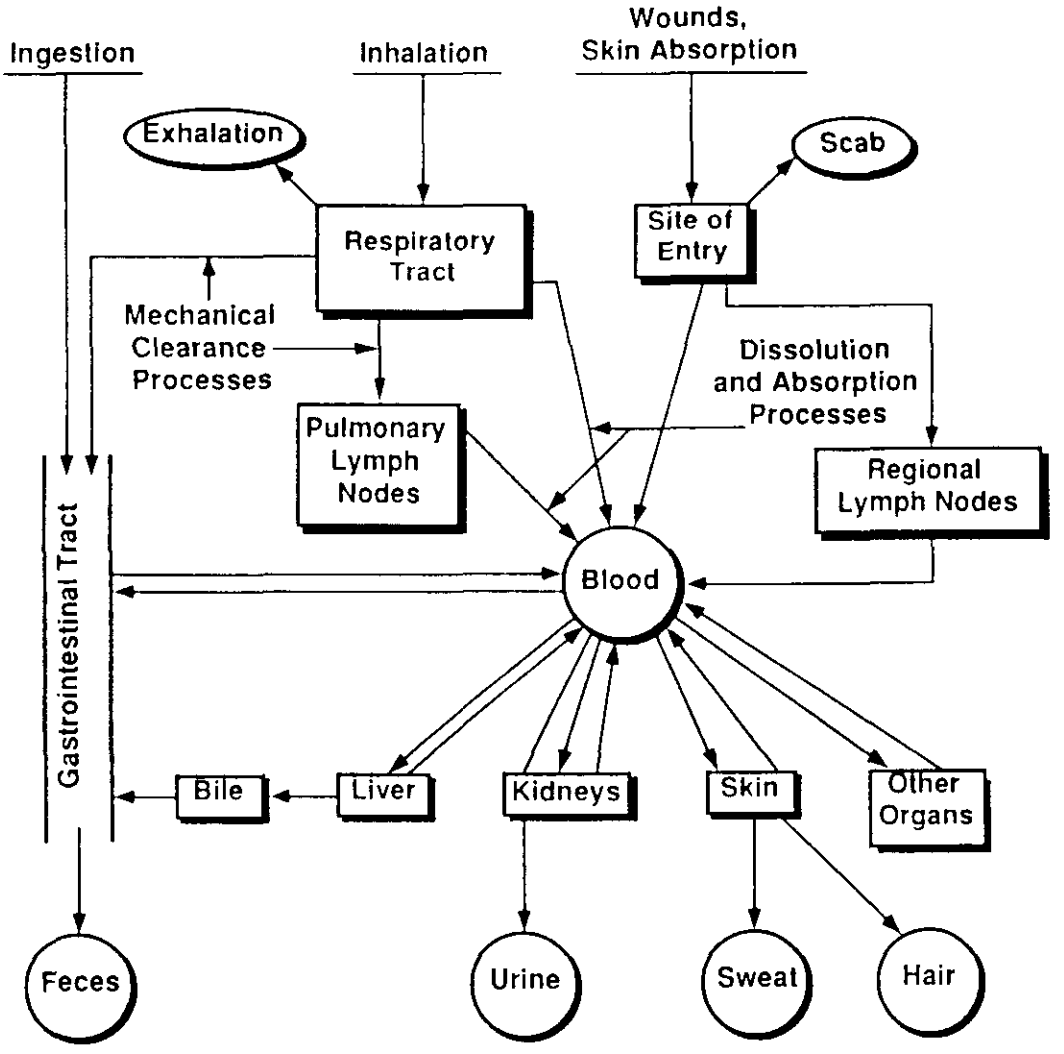

FIGURE 2-1. Schematic representation of routes of intake, metabolic behavior, and possible bioassay samples for internally deposited radionuclides (Source: Health Physics 60, Supplement 1, 45-100 (1991). Reproduced from the journal Health Physics with permission by the Health Physics Society).

regions--the nasal passage, the trachea and bronchial tree, and the pulmonary parenchyma (ICRP, 1979). A portion of the material will be deposited within the respiratory tract, with the remainder exhaled. Deposition of material varies with the aerodynamic properties of the particles composing the aerosol and with the breathing rate of the individual, as illustrated in Table 2-1 (Task Group on Lung Dynamics, 1965). In general, a portion of the deposited material will be transferred by mechanical clearance to the gastrointestinal tract and to the pulmonary lymph nodes. A portion also will be dissolved and transferred to the blood.

2. Ingestion. Radionuclides may be taken into the gastrointestinal tract by ingestion of contaminated food or water or by placing contaminated objects in the mouth. In general, a portion of the ingested material will be transferred to the blood. The remainder will be excreted in the feces, with its residence time in the gastrointestinal tract determined by the transit time for all material in the gastrointestinal tract.

3. Absorption through wounds. Radioactive material may penetrate the skin through punctures, cuts, scrapes, or other wounds. Generally, a portion of such an intake will remain at the wound site. Other portions will be absorbed into the blood, translocated to the regional lymph nodes, and removed from the body with the scab formed as the wound heals.

TABLE 2-1

Deposition of Unit Density Spheres in the Regions of the Lung

Tidal Volume	Location[a]	Diameter of Sphere (μm) 0.01	0.06	0.20	0.60
750 cm^3	N-P	0[b]	0	0	0
	T-B	0.307	0.068	0.027	0.020
	P	0.506	0.585	0.281	0.204
1450 cm^3	N-P	0	0	0	0
	T-B	0.256	0.051	0.017	0.019
	P	0.676	0.711	0.334	0.215
2150 cm^3	N-P	0	0	0	0.068
	T-B	0.208	0.035	0.015	0.021
	P	0.746	0.653	0.294	0.209

[a] N-P = Naso-pharyngeal
T-B = Tracheo-bronchial
P = Pulmonary

[b] Fraction of inhaled spheres of the indicated size deposited in the indicated region

Source: Health Physics 12, 173-207 (1966). Reproduced from the journal Health Physics with permission by the Health Physics Society.

TABLE 2-1 (Extended)

Diameter of Sphere (μm)					
1.0	2.0	3.0	4.0	6.0	10.0
0.036	0.406	0.552	0.654	0.799	0.992
0.027	0.051	0.071	0.084	0.091	0.007
0.250	0.346	0.308	0.238	0.103	0.002
0.275	0.522	0.665	0.773	0.923	1.00
0.027	0.050	0.064	0.069	0.043	0
0.242	0.330	0.250	0.150	0.033	0
0.371	0.607	0.736	0.844	1.0	1.0
0.030	0.056	0.067	0.062	0	0
0.226	0.195	0.195	0.092	0	0

4. Absorption through intact skin. A few radioactive materials, in specific chemical and physical forms, may be absorbed directly into the blood through intact skin.

After an intake by any of these routes, the rate at which the radionuclide leaves the site of intake by dissolution and absorption into the blood will depend upon the physical and chemical properties of the material of which it is a constituent.

The ICRP has developed a number of models (ICRP, 1979; ICRP, 1987) that are used to estimate the dose received by the organs of the system (such as the pulmonary region, the gastrointestinal tract, or the bones of the skeleton) resulting from an intake of radioactive material. These models were formulated to set standards for allowable intakes, based on the dose which would result from an intake of that amount. They do not contain excretion compartments and thus do not provide a direct way to calculate intake from excreta measurements (U.S. Nuclear Regulatory Commission, 1987). In fact, the ICRP cautions against using the models for purposes other than those for which they were designed (ICRP, 1979), although a later ICRP report does suggest a bioassay scheme (ICRP, 1987).

Use of Animals in Formulating Models

The development of nuclear technology and expansion of the use of radionuclides during and following World War II gave rise to the need for research on the biologic effects of internal and external exposures to radioactive materials. Such research required the development of models using animals, from which the results could be applied to man (Bustad et al., 1972). This is especially true because little information has been available on the long-term behavior in man of many internally deposited radioisotopes, especially at low levels and/or long periods of exposure. Even in cases with fairly good documentation, however, such as those available for persons who ingested radium during the early part of this century, such quantities as intake levels and material composition can only be estimated.

Rodents such as rats, mice, and hamsters have been used for many studies (e.g. Stradling et al., 1978). However, rodents may not be appropriate surrogates for human dosimetry purposes, as radionuclide retention patterns and half-times differ between rodents and man. These factors present problems in extrapolating results of the studies to man. For that reason, studies using longer-lived animals are necessary.

Nonhuman primates have been used in some studies (e.g. Durbin and Jeung, 1976). However, obtaining them and handling them are difficult and expensive. In addition, some of the

physiological characteristics of non-human primates are not as well defined as are those of other larger animals. Dogs were selected for early large-animal studies because much was known about their anatomy, physiology, and behavior; because they have a reasonably long lifespan, which can be correlated to man's; and because they are responsive to human care (Bustad et al., 1972). Beagles were determined to be an especially useful breed of dog for such studies (Goldman et al., 1986)

In some cases, the information gained from studies on animals is used qualitatively to gain a general estimation of the behavior of the material in humans. In other situations, the risk to humans for developing adverse health effects from one radionuclide can be estimated based on the associated risk in animals by assuming the risks will occur in the same ratio as those for another radionuclide, whose associated risks are known for both human and animal. For example, the risk of cancer induction due to human exposure to ^{239}Pu (for which there is very little data) has been estimated by assuming that it is proportional to the risk in dogs in the same ratio as the risk due to radium in humans is proportional to the risk due to radium in dogs (Stannard, 1990).

Plutonium-238 Biokinetic Models

Many researchers have formulated models that describe the behavior of particular elements in the body. Models developed for use after exposure to Pu include those of Langham (1950),

Beach and Dolphin (1964), Durbin (1972), the International Commission on Radiological Protection (1987), and Leggett and Eckerman (1987). However, those models were, for the most part, developed using data on exposure to ^{239}Pu. In addition, they were developed as systemic models only and do not address specifically the behavior of inhaled plutonium compounds. They also treat plutonium compounds as insoluble in the lung. Studies in beagles on the behavior of inhaled $^{238}PuO_2$ and $^{239}PuO_2$, at similar levels of radioactivity, have shown that exposure to the two materials produces different biological effects (Muggenburg, 1980; Park, 1980). Other studies have shown that $^{238}PuO_2$ is translocated from the lungs to the systemic circulation more rapidly than is $^{239}PuO_2$ (Diel and Mewhinney, 1983; Park, 1980).

The Canine Model

Mewhinney and Diel (1983) formulated a model that described the metabolism of $^{238}PuO_2$ in beagles . This model is shown schematically in Figure 2-2. The model may be divided into two main parts (Figure 2-3), one describing the behavior of inhaled material in the respiratory tract and one describing the behavior of material transferred from the respiratory tract to the bloodstream and from there to the other organs and tissues. These two major divisions are further subdivided into "compartments" representing organs and tissues and excretion routes. Because the Pu aerosols

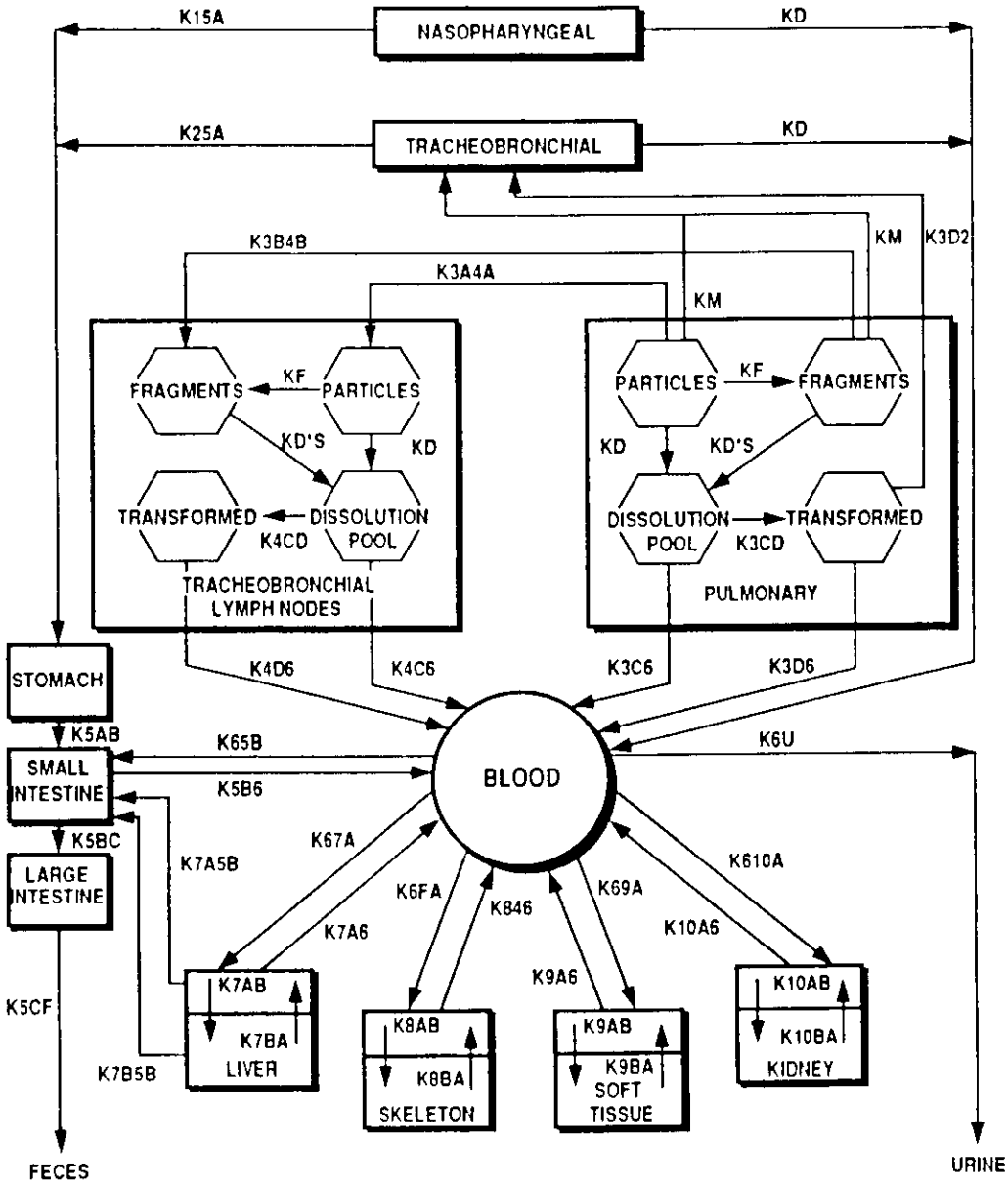

FIGURE 2-2. Schematic representation of the simulation model used to describe the metabolism and dosimetry of ^{238}Pu following inhalation of $^{238}PuO_2$ by beagles (Source: Adapted from Health Physics 45, 39-60 (1983).)

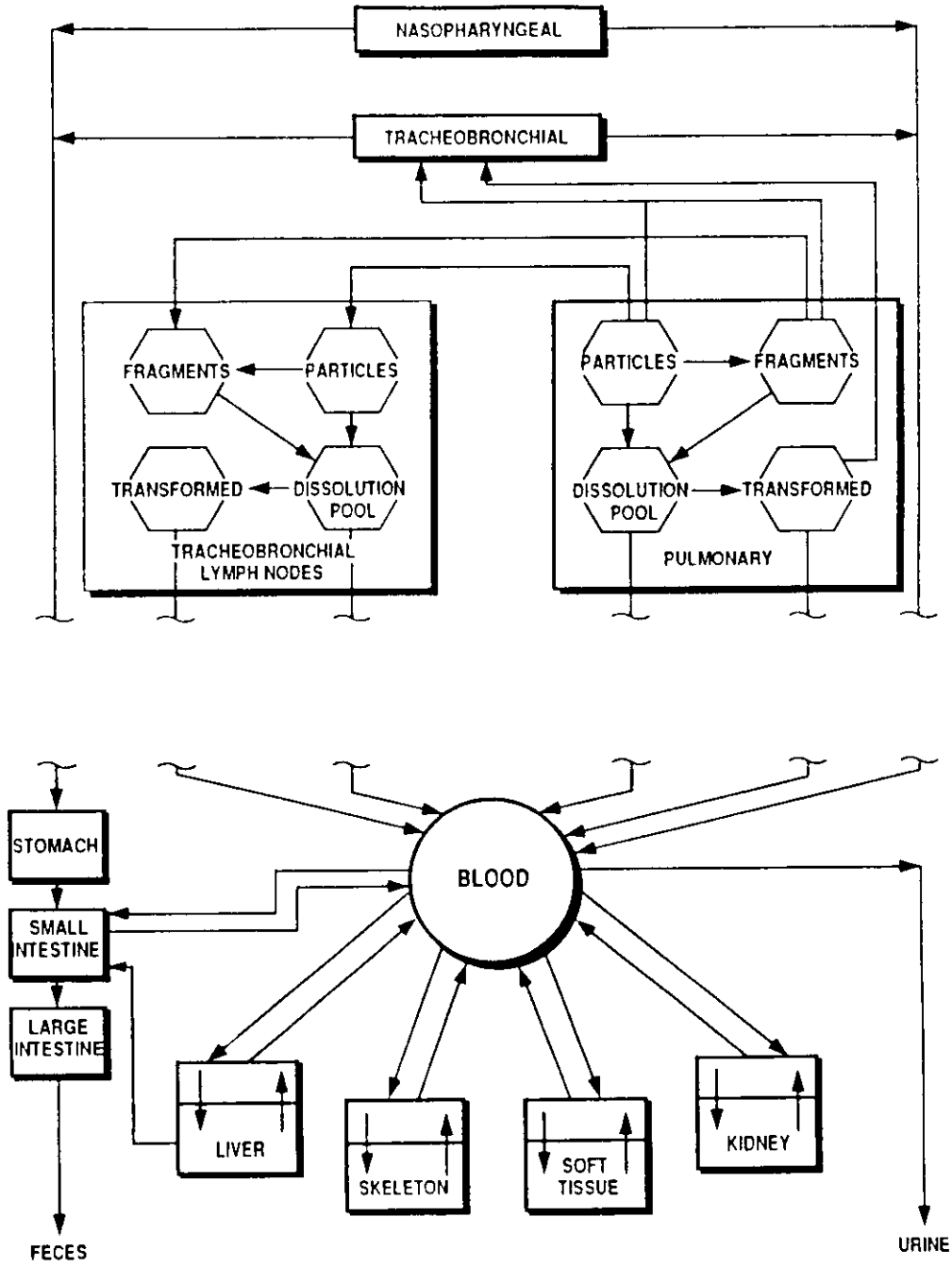

FIGURE 2-3. Division of the canine model into lung (top) and systemic (bottom) portions for modeling purposes.

examined in this study probably were insoluble at the time of inhalation and cleared rapidly from the nasopharyngeal and tracheobronchial regions with the respect to the time frames examined here (so that little or no dissolution occurs in these regions), the modeling process focused on the behavior of material deposited in the pulmonary region and the tracheobronchial lymph nodes. For that reason, the portion of the model describing the respiratory tract is referred to here as the "lung portion." That portion describing the rest of the body is referred to as the "systemic portion."

The Lung Portion

In the lung portion, the compartments represent tissues in which inhaled material may be deposited. The pulmonary and tracheobronchial lymph node compartments are further subdivided into subcompartments containing $^{238}PuO_2$ that was inhaled as particles, material that has undergone fragmentation, material that has been dissolved from particles and fragments, and material that has become bound chemically to lung constituents (that is, material retained in the lungs and lymph nodes).

The rate of particle fragmentation in the lungs is assumed to be a function of the Pu activity in the particle and the time after exposure. The fragmentation rate λ_F (KF in Figure 2-2) is

$$\lambda_P = ft^a, \quad (2)$$

where f (COEF in Table 4-1 and the appendix) is the fragmentation constant (in $days^{-a-1}$), t is the time following exposure (in days), and a is a dimensionless constant.

Plutonium-238 present as fragments is assumed to dissolve at a rate greater than that of $^{238}PuO_2$ present as particles due to the increased surface area available for dissolution processes or to be translocated mechanically to the gastrointestinal tract (and thus out of the body) or to lymph nodes. The mechanical clearance rate to the gastrointestinal tract, λ_M (KM in Figure 2-2), is

$$\lambda_M = k_1 \exp(-\gamma t) + k_2, \quad (3)$$

where k_1, k_2, and γ (EK1, EK2, and GAM, respectively, in Table 4-1 and the appendix) are constants derived from fits of the canine data.

The model uses equations developed by Mercer (1967) to describe particle dissolution as a function of their surface area. The rate at which a particle loses mass is assumed to be

$$\frac{dm}{dt} = -ks \quad (4)$$

where s is particle surface area and k (XK in Table 4-1 and the appendix) is a proportionality constant having dimensions, mass area^{-1} time^{-1}. It is further assumed that dissolved mass is removed from the vicinity of the particle quickly enough that there is no significant return of dissolved mass to the particle.

Since $s \propto m^{2/3}$, equation (4) also may be written as

$$\frac{dm}{dt} = -\alpha_s k \left[\frac{m}{\alpha_v \rho} \right]^{2/3} \tag{5}$$

where $\alpha_s = s/D^2$ = the surface shape factor,

$\alpha_v = m/\rho D^3$ = the volume shape factor,

ρ = the particle density, and

D = the particle diameter.

The first three variables are ALS, ALV, and DEN in Table 4-1 and the appendix. The two shape factors are assumed to remain constant as the particle dissolves.

At any time t after dissolution begins and before it is complete, the mass of the particle is

$$m = m_0 \left[1 - \frac{\alpha_s k t}{3 \alpha_v \rho D_0} \right]^3 \tag{6}$$

where m_0 is the initial particle mass and D_0 is the initial diameter. The particle mass will be reduced from some mass m_1 to $m_2 = 0.5\ m_1$ in time $t_2 - t_1$, where

$$t_2 - t_1 = 0.206 \left[\frac{3 \alpha_v \rho D_0}{\alpha_s k} - t_1 \right]. \tag{7}$$

The half-life of a single particle (or a population of monodisperse particles satisfying the same assumptions), measured from t_1, will diminish linearly with time. The particle is assumed to dissolve completely at $t = 3\alpha_v \rho D_0 / \alpha_s k$.

A population of particles initially having a log-normal size distribution can be characterized by a mass median diameter, D_m (XMMD in Table 4-1 and the appendix), and a geometric standard deviation, σ_g (SIGG in Table 4-1 and the appendix). Consider now a population of such particles in a suspension satisfying the above mentioned assumptions concerning particle dissolution kinetics, removal of mass from the particle vicinity, and total dissolution time. If the initial mass of the entire population is M_0, then at any time t the total mass remaining undissolved will be

$$M = (M_0/\sigma\sqrt{2\pi}) \int_{x_t}^{\infty} (m/m_0) \exp\{-(x - x_m)^2/2\sigma^2\}\, dx \qquad (8)$$

where $x = \ln D$, $x_m = \ln D_m$, $x_t = \ln D_t$, D_t is the initial diameter of the largest particle which will dissolve completely in time t, and $\sigma = \ln \sigma_g$.

Substituting m/m_0 from equation (6) into equation (8) and integrating yields

$$M/M_0 = \sum_{i=0}^{3} K_i \int_{Y_i}^{\infty} f(y)\,dy \qquad (9)$$

where $f(y) = (2\pi)^{-1/2}\exp(-y^2/2)$

$K_0 = 1$

$K_1 = -\beta \exp 0.5\,\sigma^2$

$K_2 = (\beta^2/3) \exp 2\,\sigma^2$

$K_3 = -(\beta^3/27) \exp 4.5\,\sigma^2$

$\beta = \alpha_v kt/\alpha_v \rho D_m$

$Y_i = (1/\sigma) \ln (\beta/3) + i\sigma.$

The Systemic Portion

Organs and tissues other than the lungs, as well as excretion pathways, are contained in the systemic portion of the model. The blood is represented as a transfer compartment into which dissolved material enters from the pulmonary and lymph node compartments and out of which Pu is distributed to the other organs and tissues and directly to urine. Organs other than the gastrointestinal tract are represented by two compartments, one for transfer of Pu to and from the blood and the other for internal storage of Pu. These other organ compartments include the skeleton and liver, principal sites of ^{238}Pu deposition; the kidneys, through which Pu passes as a part of urinary excretion; and a miscellaneous soft tissue compartment. The liver also contains a pathway for excretion of Pu directly to the small intestine via the bile. The gastrointestinal tract is represented as a one-way path out of

the body, with Pu entering it via mucociliary clearance from the lungs, biliary excretion from the liver, and direct translocation from the blood. Feces and urine are also one-way paths; fecal Pu comes from the GI tract, and urinary Pu comes directly from the blood.

CHAPTER 3
METHODOLOGY

The model of Mewhinney and Diel (1983) was developed using data obtained from inhalation exposures to $^{238}PuO_2$. It was therefore of interest in this study to apply the model to other canine studies before applying it to human data. A study of the metabolism of injected $^{239}PuO_2$ (Stover et al., 1959) was selected as the source of comparison data. Data of interest included concentration of ^{239}Pu in plasma (as percentage of injected dosage per gram of plasma) and urinary excretion of ^{239}Pu (as percentage of injected dosage excreted per day). As the data were available only in graphic form, a method described by Guilmette and Mewhinney (1989) was used to obtain numeric values. Individual data points were digitized, using a sonic digitizer (Graf Pen) coupled to a VAX 11/780 computer to obtain per cent of injected activity present and time after exposure. The digitization was performed only once as only a general idea of goodness of fit was desired.

The average mass of the dogs used by Stover et al. was 9.0 kg, and the average plasma volume was 49.3 ml/kg body mass. Thus, percentage of injected dosage/gram plasma is easily converted to percentage injected dosage present in the blood at any time after injection. This conversion allows the

results of a simulated injection exposure to be compared to the data of Stover et al. (1959).

Applying the metabolic model for an injection exposure, with a radioactive decay constant of 7.9×10^{-8} d^{-1} for ^{239}Pu ($t_{1/2} = 2.4 \times 10^{4}$ y) (Walker at al., 1989), produced reasonable agreement, in light of the method of comparison used and the general variability seen among biologic organisms. Having established that the canine model was applicable to conditions other than those under which it was formulated, attention was turned to modifying it for use with human data.

Peak excretion of ^{238}Pu occurs several hundred days later in the exposed humans than was seen for the beagles. Therefore, at least some of the rate constants governing transfer of the inhaled Pu between organ compartments required modification. In addition, as the characteristics of the aerosol inhaled by the humans were not available, it was not unreasonable to modify at least some of these values to examine their effect on the excretion curve.

Changes to the Lung Portion

The division of the canine model into lung and systemic portions (Figure 2-3) is convenient when analyzing the rate constants and aerosol characteristics. Attention first was focused on the lung portion of the model. Because the aerosol characteristics were not available, the effects of changing these values on the shape of the urinary excretion curve were

investigated first. Both particle solubility and geometric standard deviation of particle mass median diameter affect the rate of dissolution of particles and fragments. Particle solubility was varied by factors of 2 and 10 greater and less than the values from the canine model and geometric standard deviation, which influences the dissolution rate of particles and fragments, was varied from 1.1 (i.e., ± 10%) to 2.0 (± 100%) to investigate the sensitivity of the urinary excretion curve to these changes.

Particle mass median diameter, surface and volume shape factors, and density also affect the dissolution rate. However, according to Mercer (1967), the effects of solubility and mass median diameter are inversely related, as in

$$m = m_0 \left[1 - \frac{\alpha_s k t}{3 \alpha_v \rho D_0} \right]^3 , \qquad (6)$$

so that, for example, doubling one should produce the same effect as halving the other. Thus, the trend seen by varying solubility should be the inverse of that seen by varying mass median diameter. Particle density and shape factors are less likely to vary than are the other characteristics and so were not examined.

The dissolution rate of the fragments is assumed to be

$$\lambda_{D(frag)} = \lambda_{D(part)} \cdot S \qquad (10)$$

where $\lambda_{D(frag)}$ = dissolution rate constant for fragments,

$\lambda_{D(part)}$ = dissolution rate constant for particles, and

S = increased surface area of fragments over particles.

Because the factor S may depend on the initial particle size, the effect of varying this value was investigated.

The effects of changes in the fragmentation rate,

$$\lambda_p = ft^{-a}, \qquad (11)$$

were investigated as well. In addition to studying changes in the variables f and a individually, the effect of coupling the two and changing both was examined. This was done because the variable a is an exponent, and changing it causes a more complex change in the fragmentation rate than does changing f. The variables f (canine model value 5×10^{-4}) and a (canine model value 0.48) were coupled so that $ft^{-a} = 1$ for all selected combinations of f and a at time $t = (5 \times 10^{-4})^{-1/0.48}$ d after inhalation. Table 3-1 lists all values of the variables tested. The effects of changing the rate of mucociliary clearance and those rate constants not dependent upon time were not tested.

TABLE 3-1

Values of Selected Variables Tested for Their Effects on the Shape of the Excretion Curve

Variable	Values Tested				
Particle Solubility Constant k ($g\ cm^{-2}\ d^{-1}$)	2.5×10^{-9}	1.25×10^{-8}	2.5×10^{-8} *	5×10^{-8}	2.5×10^{-7}
Relative Surface S	2	10	20*	40	200
Uncoupled Fragmentation Rate Variables f (d^{-a-1})	5×10^{-5}	2.5×10^{-4}	5×10^{-4} *	1×10^{-3}	5×10^{-3}
a	0.25	0.48*	1.0	1.5	2.0
Coupled Fragmentation Rate Variables f (d^{-a-1})	1.9×10^{-2}	5×10^{-4} *	1.3×10^{-7}	4.8×10^{-11}	1.8×10^{-14}
a	0.25	0.48*	1.0	1.5	2.0
Particle Diameter Geometric Standard Deviation σ_g	1.1	1.5	2.0*		

* Canine model values

Changes to the Systemic Portion

After examining changes to the lung portion of the model, attention was turned to modifying the systemic portion of the model to reflect knowledge of the behavior of Pu in humans. The systemic rate constants used in the canine model gave retention half-times for both liver and skeleton of about 6 y. The ICRP has published two sets of retention half-times for Pu in these organs. The older numbers (ICRP, 1979) are 40 y for the liver and 100 y for the skeleton. The more recent values (ICRP, 1987) are 20 y and 50 y, respectively. Several recent studies (McInroy et al., 1989; Kathren and McInroy, 1991; McInroy et al., 1991) of whole bodies donated to the United States Transuranium Registry (USTR) indicate that the earlier ICRP half-times are more appropriate for the systemic behavior of ^{239}Pu, and this relationship should apply to ^{238}Pu as well. Initial partitioning of ^{238}Pu among the organs was taken to be that seen by McInroy et al (1989) in their earlier study and was as follows:

Liver	45%
Skeleton	45%
Soft Tissue	4%
Kidneys	0.4%.

A ratio of (activity in urine/activity in feces) of 1 was proposed based on Leggett's work (1985).

Adjusting only the rate constants into and out of the first ("A") compartments of the organs provided either the

desired Pu residence half-times or the desired ratio of (activity in urine/activity in feces), but not both. Therefore, adjusting the rate constants governing transfer between the first and second ("B") compartments proved necessary.

The modeling process used in this work involved first identifying model variables that were candidates for modification and likely values for these variables and then testing the effects of changing the variable values. To be acceptable, a change in a value had to result both in a better fit of the predicted urinary excretion curve to the human data and in metabolic behavior (such as retention half-times in organs) consistent with existing knowledge on the behavior of Pu in humans (except where the excretion data indicated otherwise).

The procedure used in this study involved simulating an injection exposure to ^{238}Pu to analyze the effect of changes in variable values on the metabolic behavior of Pu and then simulating an inhalation exposure to determine the effect of those changes on the excretion curve. Further changes then were analyzed for their effects on first the excretion curve (inhalation simulation) and then the metabolic behavior (injection simulation). During this analysis, excretion data used were normalized to a point as close to 971 d post exposure as the data allowed. This point was selected because excretion had reached its peak by this time and because data

were available on this day for four of the cases and within 14 d of it for the other three.

This process was repeated until a simulated inhalation exposure produced urinary excretion curves that provided a good fit by eye to the data and a simulated injection exposure produced metabolic characteristics consistent with those seen in previously reported cases of human exposure. Initial lung burdens were then estimated by fitting the excretion curve to the actual data for various values of ILB for each case. To compare the model predictions with behavior seen by other investigators, the urinary excretion pattern produced by a simulated injection exposure to ^{239}Pu was compared to data from the studies by Langham et al (1950) and Leggett and Eckerman (1987). The results are reported in the next chapter.

CHAPTER 4
RESULTS AND CONCLUSIONS

Effects of Changes in Aerosol-Associated Variables

The results of varying aerosol characteristics and the parameters associated with the fragmentation rate are shown in figures 4-1 to 4-6. Variation in particle size distribution (Figure 4-1) had little effect on the shape of the excretion curve for the mass median particle diameter (4.8×10^{-5} cm) assumed in the canine model, with urinary excretion being only slightly higher for the larger size distributions (approximately 7×10^{-4} % inhaled activity for $\sigma_g = 2.0$ vs. approximately 5.5×10^{-4} % for $\sigma_g = 1.1$). The excretion curves come together at approximately 300 d post exposure, when peak excretion is occurring. This lack of influence is due to the small size of the inhaled particles.

Increasing the relative surface area of fragments over particles, S, resulted in increased excretion (Figure 4-2), with peak excretion occurring earliest for the maximum value of relative surface area (10^{-2} % inhaled activity at approximately 150 d post-exposure for S = 200 vs. 4×10^{-3} % at 2000 d post-exposure for S = 2). This occurs because increased surface area allows for faster dissolution of fragments and thus enhanced translocation of Pu from lung to

FIGURE 4-1

Effect of varying size distribution (geometric standard deviation, σ_g) of inhaled particles on predicted daily urinary excretion of ^{238}Pu for humans

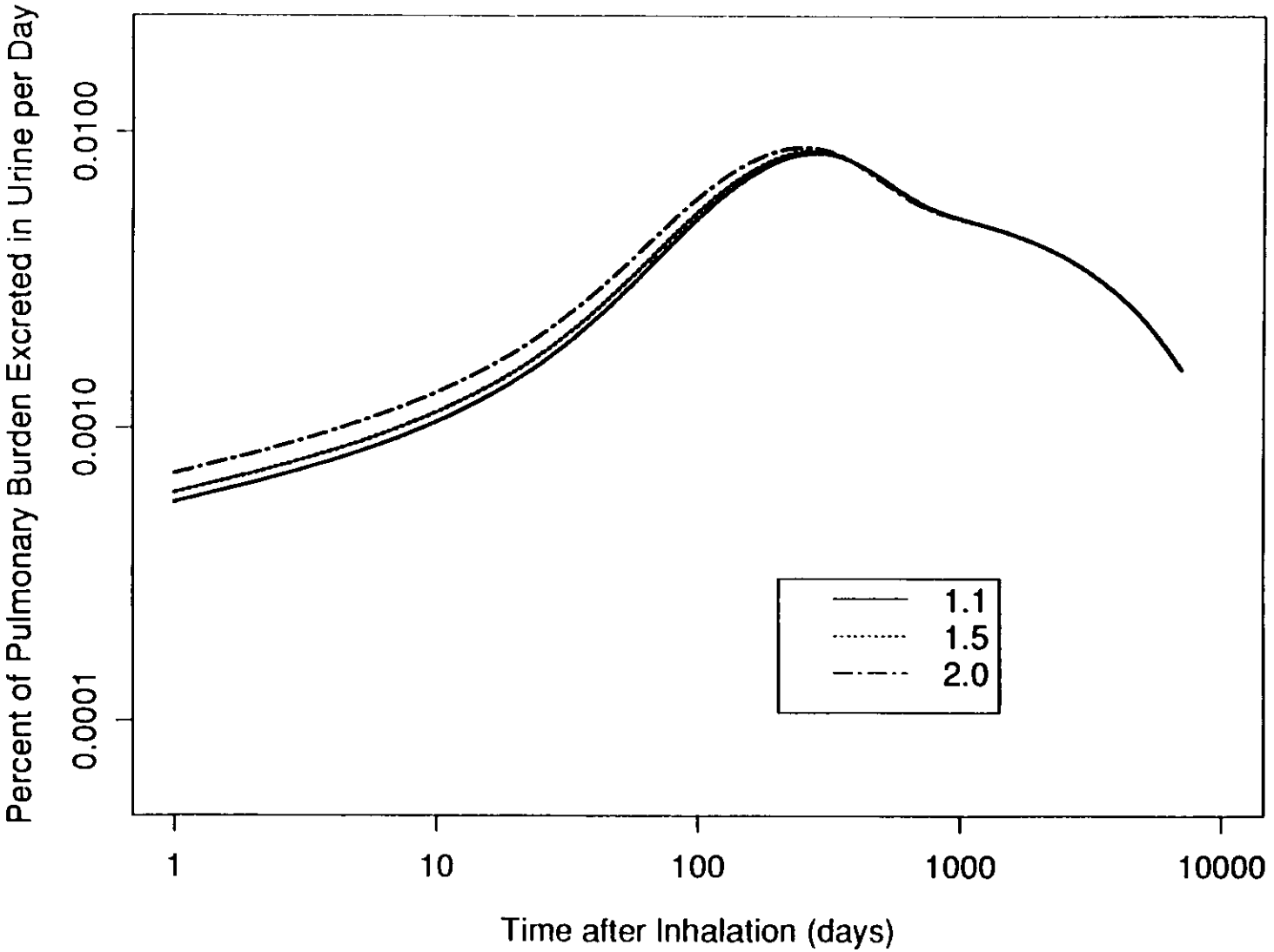
Percent of Pulmonary Burden Excreted in Urine per Day
0.0100
0.0010
0.0001
1
10
100
1000
10000
Time after Inhalation (days)
1.1
1.5
2.0

FIGURE 4-2

Effect of varying surface area of fragments relative to surface area of inhaled particles (S) on predicted daily urinary excretion of ^{238}Pu for humans

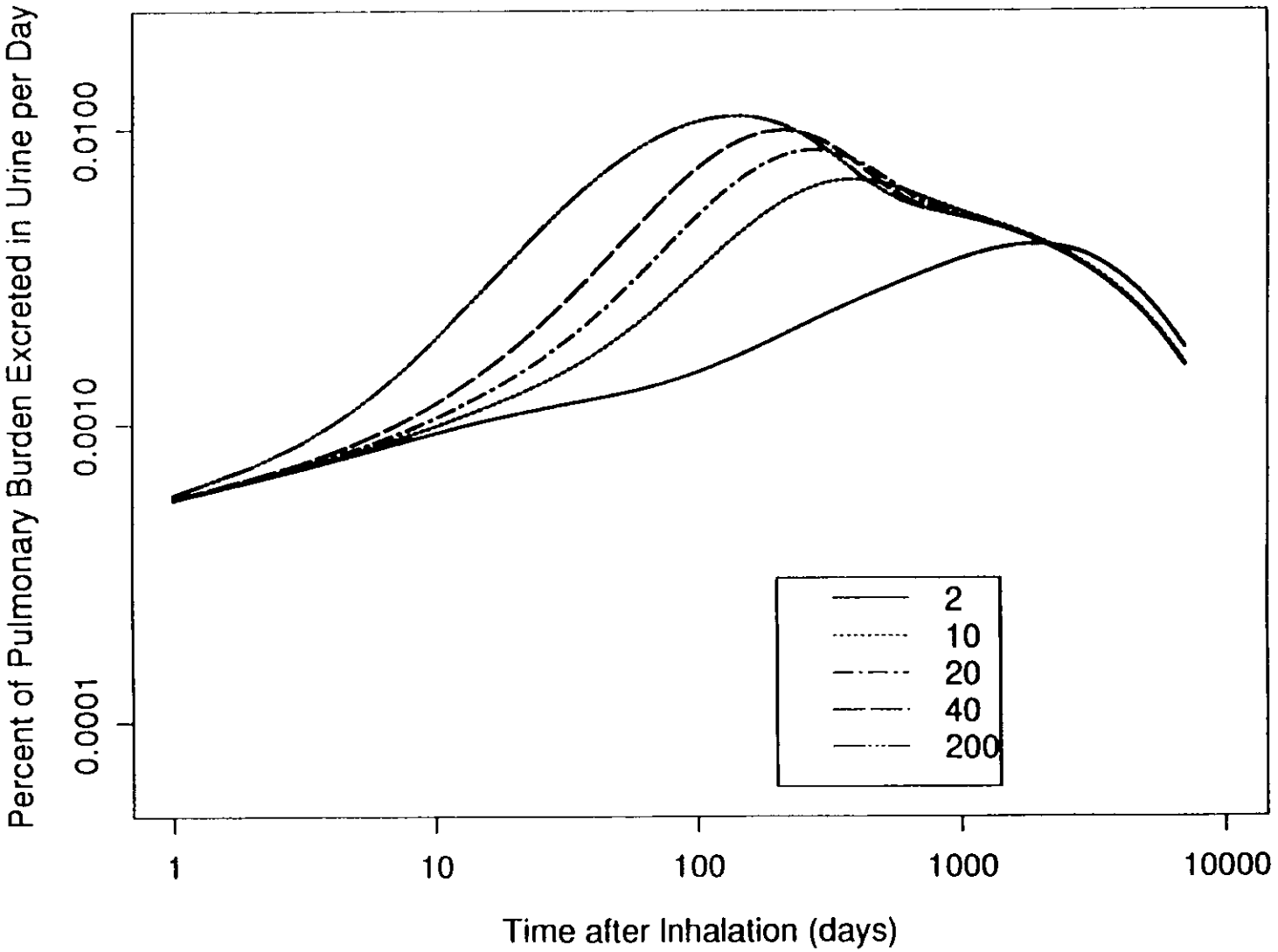
Percent of Pulmonary Burden Excreted in Urine per Day
0.0001
0.0010
0.0100
1
10
100
1000
10000
Time after Inhalation (days)
2
10
20
40
200

FIGURE 4-3

Effect of varying fragmentation rate parameter f for inhaled particles on predicted daily urinary excretion of ^{238}Pu for humans

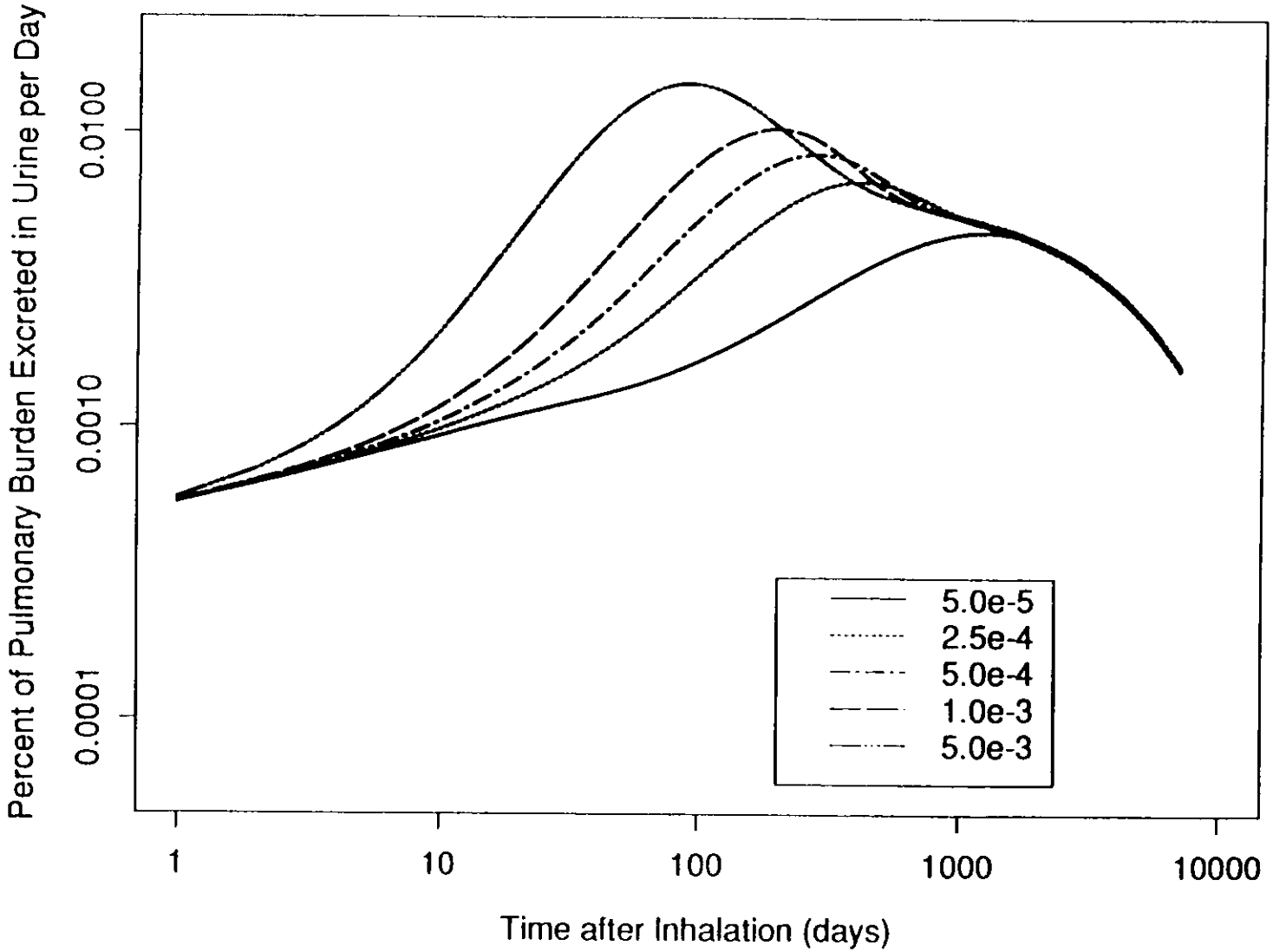
Percent of Pulmonary Burden Excreted in Urine per Day
0.0100
0.0010
0.0001
1
10
100
1000
10000
Time after Inhalation (days)
5.0e-5
2.5e-4
5.0e-4
1.0e-3
5.0e-3

FIGURE 4-4

Effect of varying fragmentation rate parameter a for inhaled particles on predicted daily urinary excretion of ^{238}Pu for humans

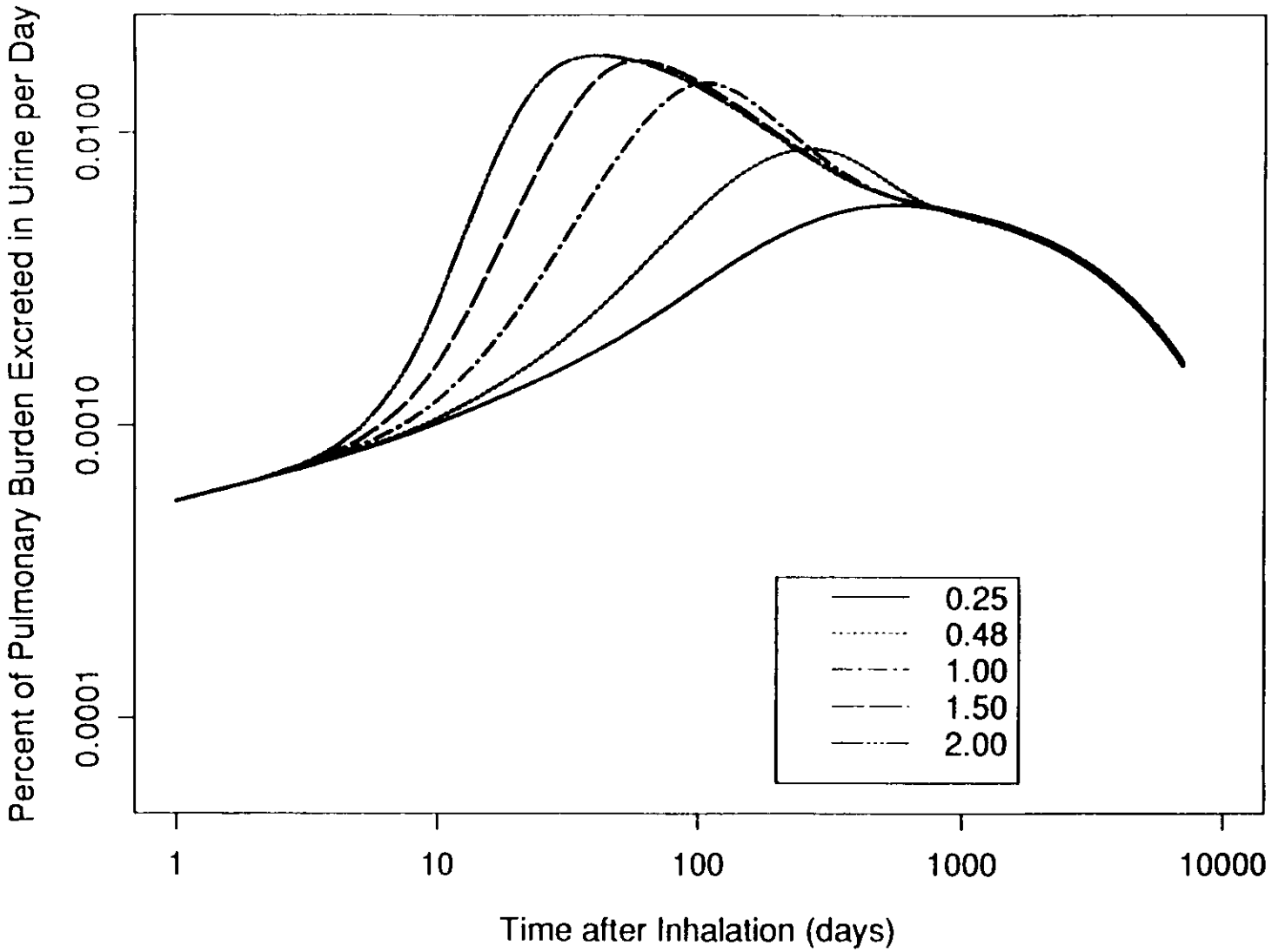
Percent of Pulmonary Burden Excreted in Urine per Day
0.0100
0.0010
0.0001
1
10
100
1000
10000
Time after Inhalation (days)
0.25
0.48
1.00
1.50
2.00

FIGURE 4-5

Effect of varying in tandem fragmentation rate parameters f and a for inhaled particles on predicted daily urinary excretion of ^{238}Pu for humans

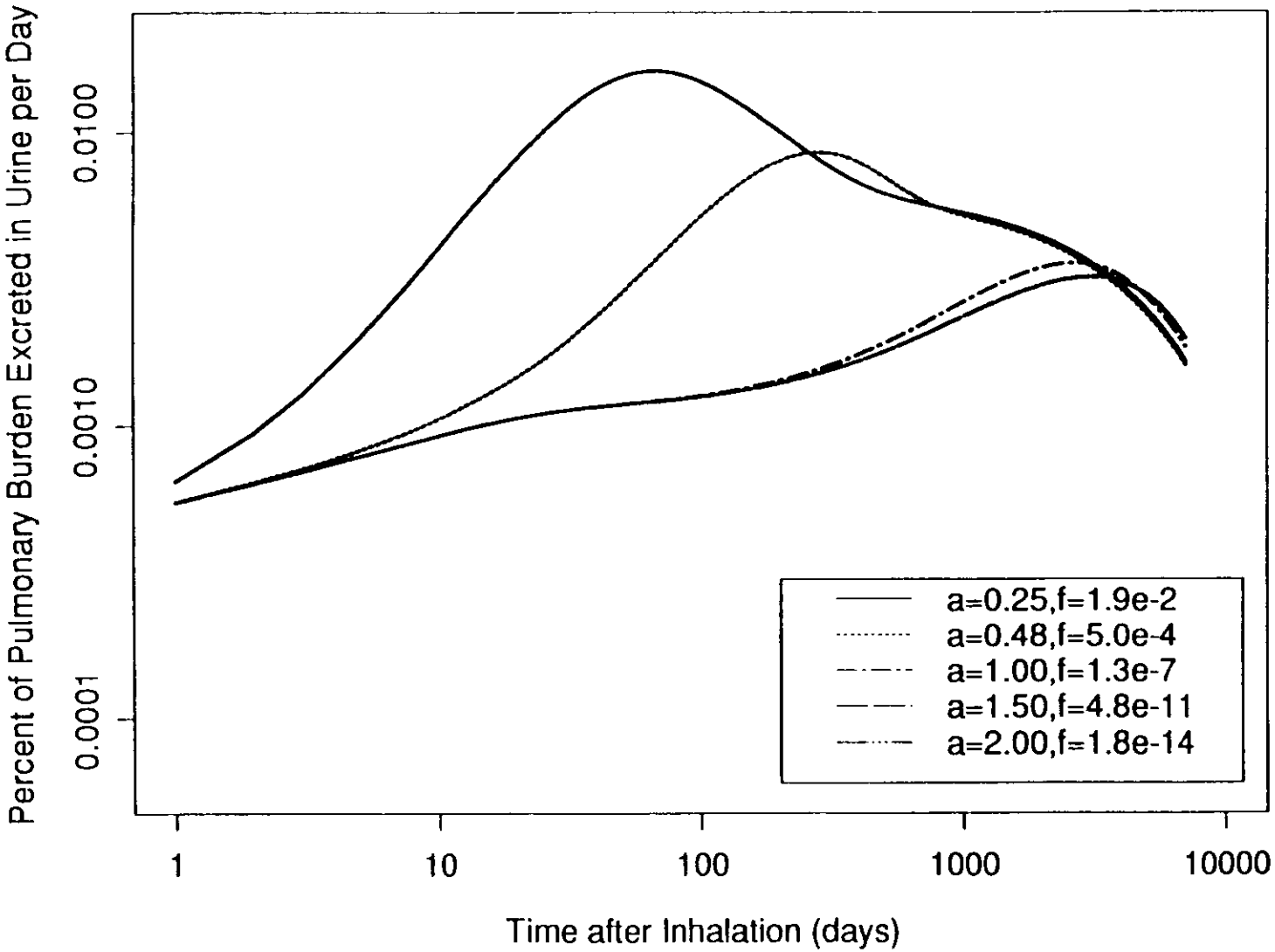
Percent of Pulmonary Burden Excreted in Urine per Day
0.0100
0.0010
0.0001
1
10
100
1000
10000
Time after Inhalation (days)
a=0.25,f=1.9e-2
a=0.48,f=5.0e-4
a=1.00,f=1.3e-7
a=1.50,f=4.8e-11
a=2.00,f=1.8e-14

Page 52
missing
from original.

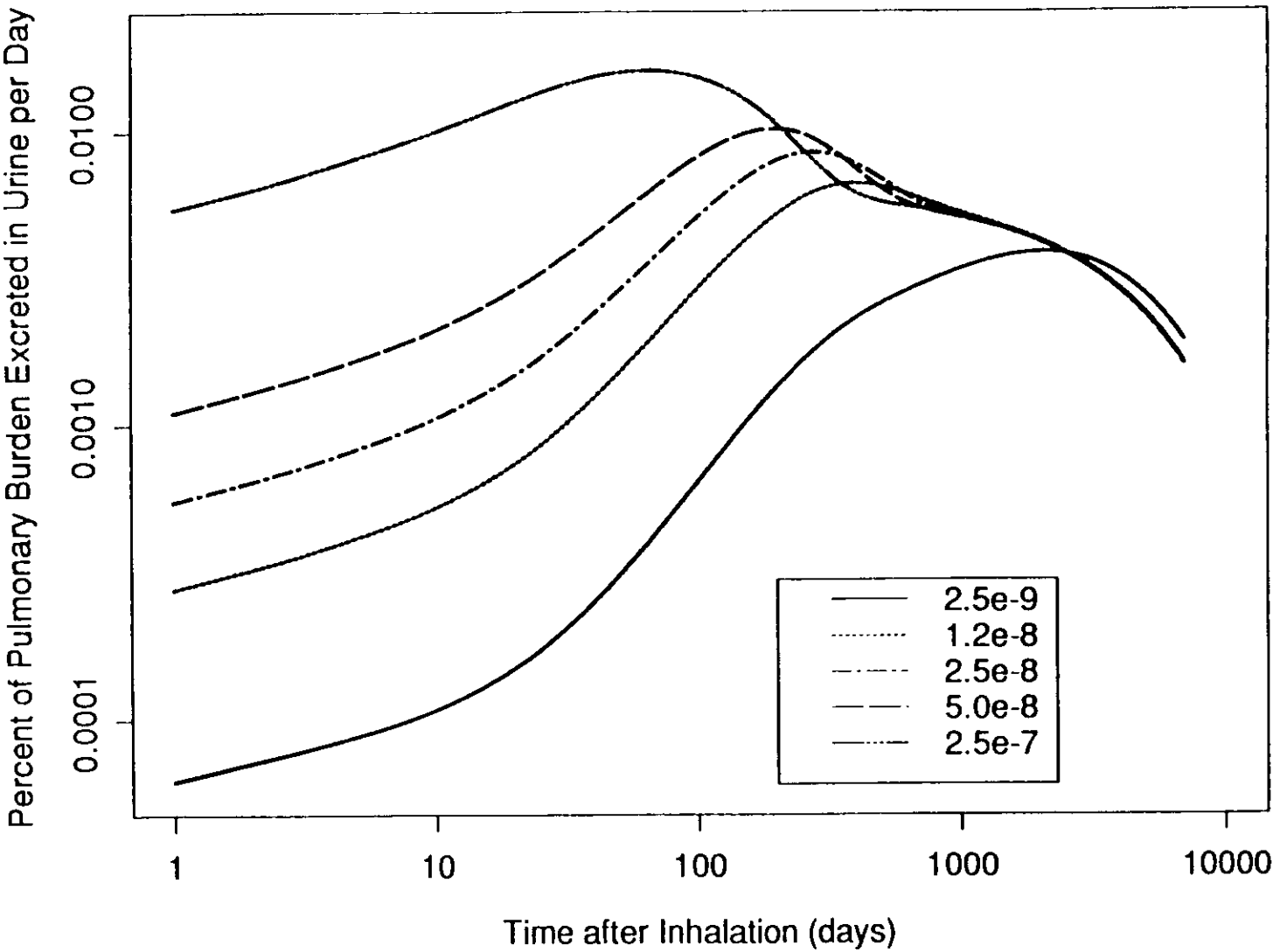
Percent of Pulmonary Burden Excreted in Urine per Day
0.0001
0.0010
0.0100
1
10
100
1000
10000
Time after Inhalation (days)
2.5e-9
1.2e-8
2.5e-8
5.0e-8
2.5e-7

blood. However, time to peak excretion is noticeably longer for S = 2 than was expected from the trend for the other values.

The patterns and trends observed from varying the fragmentation rate parameters f and a individually (enhanced excretion and earlier peak excretion times for increased values of the variables) were similar to those observed for S (figures 4-3 and 4-4). When the two were varied in tandem (Figure 4-5), excretion was markedly enhanced for $\lambda_f = 1.9 \times 10^{-2}\ t^{0.25}$ over the canine model value of $\lambda_f = 5 \times 10^{-4}\ t^{0.48}$ (peak excretion 1.5×10^{-2} % at 70 d post-exposure vs. 8×10^{-3} % at 300 d post-exposure). Likewise, excretion was markedly decreased for the other values of λ_f (peak excretion approximately 3×10^{-3} % at 3000 d post-exposure). Thus it seems that f is the dominant factor in determining fragmentation rate.

Effects of varying solubility are shown in Figure 4-6. In addition to influencing peak excretion levels and times, changes in solubility also affected initial excretion levels. Increased particle solubility would result in higher initial excretion, and vice versa. However, it is significant that only solubility had this effect. This seems to imply that the increased surface area of the fragments over the particles does not enhance translocation of Pu (and thus excretion) until some time has elapsed following inhalation.

Early simulations produced estimates of initial excretion that were too high. One possible explanation is that damage to the particles might not reach a level sufficient to cause fragmentation until several days following exposure. However, introducing a time delay into the fragmentation process (i.e. making $\lambda_f = f(t-d)^a$, where d = time in days required for fragmentation to begin) had no discernible effect on the shape of the excretion curve. Thus, the solubility of the particles inhaled by the workers (set at 3×10^{-10} g cm^{-2} d^{-1}) was assumed to be less than that of the particles inhaled by the dogs used in developing the model (2.5×10^{-8} g cm^{-2} d^{-1}).

In order to maintain the rate of fragment dissolution at the level seen in the earlier human simulations (which provided good fits to the excretion data for times after about 30 d), S was increased from 20 to 200. The rate of fragmentation was increased as well, by increasing f to 1×10^{-3} from the canine value of 5×10^{-4}. None of the other lung-associated variables or rate constants were modified.

Effects of Changes in Systemic Rate Constants

Most of the systemic rate constants were changed from the values of the canine model. A comparison of all aerosol characteristics and rate constants for the original and modified models is given in Table 4-1. In addition, an additional transfer pathway was added from the first ("A") liver compartment to the small intestine. This was done to

TABLE 4-1

Comparison of Variable Values in the Canine and Human Models

Variable	Canine Model Value	Human Model Value
Radioactive Decay Constant (d^{-1})		
TC	2.16×10^{-5} [a]	2.16×10^{-5}
Intercompartmental Rate Constants (d^{-1})		
K15A	20.	20.
K25A	20.	20.
K3A4A	2×10^{-3}	2×10^{-3}
K3B4B	4×10^{-3}	4×10^{-3}
K3CD	10.	10.
K3C6	90.	90.
K3D2	2×10^{-3}	2×10^{-3}
K3D6	1×10^{-4}	1×10^{-4}
K4CD	10.	10.
K4C6	90.	90.
K4D6	2×10^{-3}	2×10^{-3}
K5AB	15.	15.
K5BC	5.0	5.0
K5B6	1×10^{-3}	1×10^{-3}
K65B	0.	0.
K5CF	100.	4.
K67A	1.1	0.6
K7A6	0.07	1.9×10^{-3}
K7AB	0.09	1.9×10^{-4}
K7BA	5×10^{-3}	7.6×10^{-5}
K7A5B	N/P[b]	9.4×10^{-5}
K7B5B	2×10^{-4}	4.7×10^{-5}

TABLE 4-1 (continued)

Variable	Canine Model Value	Human Model Value
K68A	1.1	0.6
K8A6	0.07	1.9×10^{-3}
K8AB	0.10	1.9×10^{-4}
K8BA	6×10^{-3}	5.4×10^{-5}
K69A	1.1	1.0
K9A6	0.55	0.05
K9AB	0.03	5×10^{-3}
K9BA	5×10^{-3}	1.9×10^{-3}
K610A	0.02	5×10^{-3}
K10A6	0.06	1.9×10^{-3}
K10AB	0.03	0.03
K10BA	6×10^{-3}	1.9×10^{-3}
K6U	0.05	0.06
K10AU	N/P	0.
Activity Partitioning Factor		
BLOOD	N/P	1.0
Dissolution Rate Constant-Associated Variables		
S	20.	200.
ALS	6.0	6.0
ALV	1.0	1.0
XK ($g\ cm^{-2}\ d^{-1}$)	2.5×10^{-8}	3×10^{-10}
DEN ($g\ cm^{-3}$)	8.0	8.0
XMMD (cm)	4.8×10^{-5}	4.8×10^{-4}
SIGG	1.1	1.1

TABLE 4-1 (Continued)

Variable	Canine Model Value	Human Model Value
Mechanical Clearance Rate Constant-Associated Variables		
EKM1 (d^{-1})	0.03	0.03
GAM	0.3	0.3
EKM2 (d^{-1})	8×10^{-4}	8×10^{-4}
Fragmentation Rate Constant-Associated Variables		
COEF (d^{-A-1})	5.0×10^{-4}	1×10^{-3}
A	0.48	0.48

[a] Radioactive decay constant for ^{238}Pu

[b] N/P = Not present in the canine model but added for the human model

achieve the desired ratio of urine to feces activity ratio. The SimuSolv code as modified for humans appears in the Appendix.

Effective retention half-times for Pu in the skeleton and liver for simulations of three combinations of isotope and exposure route are listed in Table 4-2. Biological half-times are listed as well and are computed by

$$T_B = \frac{T_P\, T_E}{T_P - T_E} , \qquad (12)$$

where T_B = Biological half-life,

T_P = Physical half-life, and

T_E = Effective (retention) half-life.

TABLE 4-2

Physical Half-Life and Predicted Effective and Biological Half-Times for Pu in Liver and Skeleton for Three Isotope-Exposure Route Combinations

Isotope and Exposure Route	T_P (y)	Skeleton		Liver	
		T_E (y)	T_B (y)	T_E (y)	T_B (y)
^{238}Pu (Inhalation)	87.7	44	88	22	29
^{238}Pu (Injection)	87.7	51	122	21	28
^{239}Pu (Injection)	2.4×10^4	112	113	46	46

T_P = Physical half-life

T_E = Effective retention half-time

T_B = Biological half-time

Although there is much variability, results for retention in skeleton correspond more closely to the older ICRP (1979) value of 100 y. Results for retention in liver are less conclusive. The biological half-life of ^{239}Pu is closer to the older ICRP value of 40 y, while that of ^{238}Pu seems to be closer to the newer value of 20 y (ICRP, 1986). Kathren et al. (1988) noted a possible isotope effect in the partitioning of Pu between liver and skeleton, although they note that it might have been an artifact of the data. In this study, difficulties in modeling the liver, associated in part with a lack of fecal data, may account for the observed differences in biological half-lives.

In order to produce an excretion curve that matched that seen in the human data and to maintain the desired urine-to-feces ratio, the soft tissue was forced to take up Pu from the blood and return it to the blood fairly rapidly. This resulted in the soft tissue receiving a large share of the inhaled activity initially (about 38%, vs. only about 25% to both liver and skeleton). However, by 100 d after exposure, the partitioning of activity was approximately that seen in the studies of workers exposed to ^{239}Pu:

Skeleton	42 %
Liver	42 %
Soft Tissue	10 %
Kidneys	0.38%.

At 10^4 d after injection of ^{239}Pu, partitioning among the organs was

Skeleton	64%
Liver	33%
Soft Tissue	2%
Kidneys	0.5%,

which agrees well with results reported by McInroy et al. (1989) for partitioning at long times after exposure in five whole bodies donated to the USTR of

Skeleton	53.7 ± 12.5%
Liver	35.4 ± 12.5%
Muscle	6.5 ± 1.8%
Other	4.4 ± 1.7%.

Application of the Modified Model to the Human Data

The urinary excretion curve produced by the modified model is plotted with the data from each of the seven individuals in figures 4-7 to 4-13. Because the workers identified as Case 3 and Case 6 had the highest intakes, more and earlier data points were available for them than for the other workers. Therefore, the modeling process depended more heavily on these data in fitting the excretion curves, and this is reflected in the fit of the final curves. However, even for those cases with lower exposure and fewer data points, the fit of the predicted urinary excretion curve to the data is good.

FIGURE 4-7

Prediction of the simulation model, as modified for use with human data, for daily urinary excretion of ^{238}Pu for Case 1

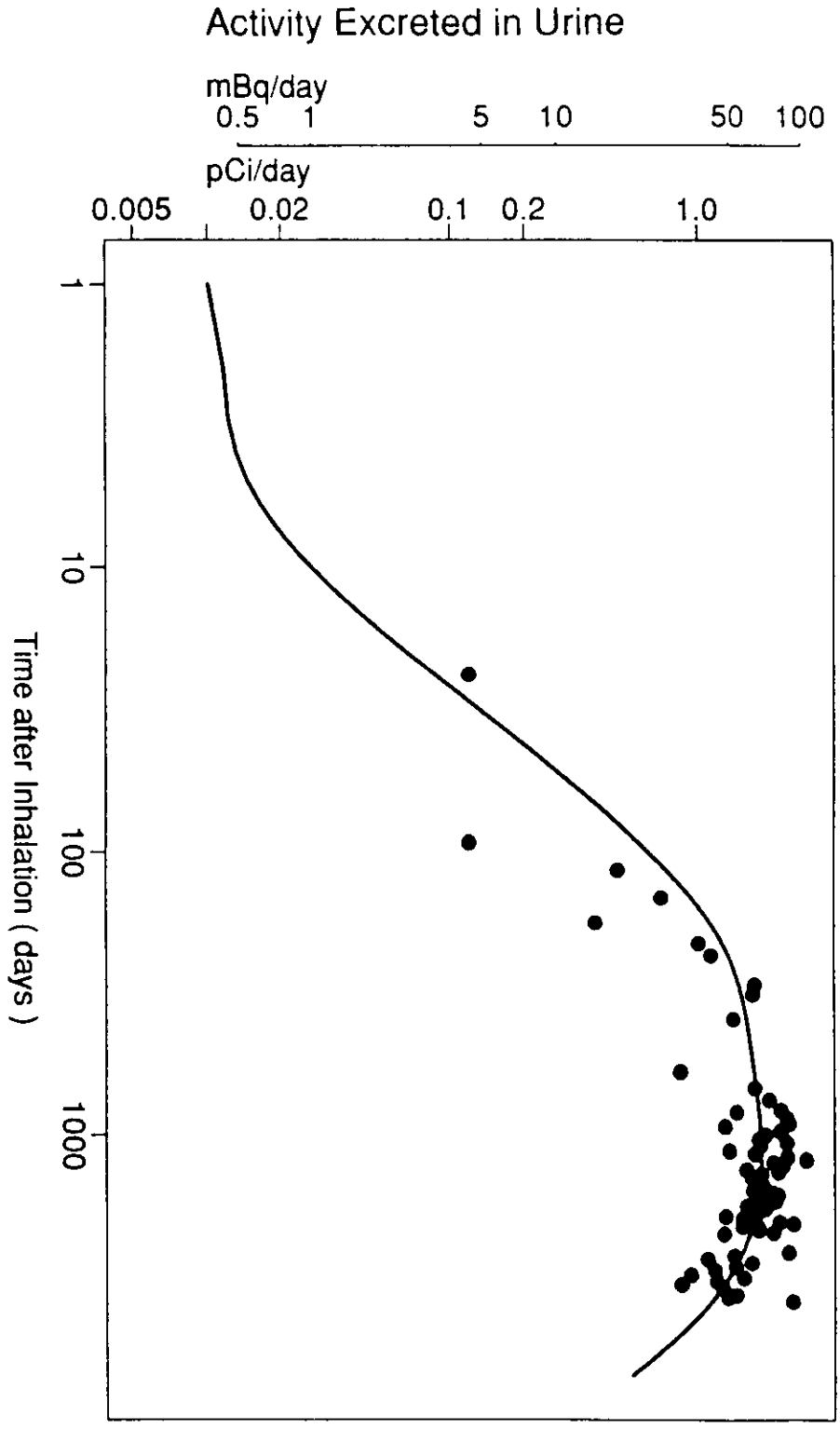
Activity Excreted in Urine
mBq/day
0.5
1
5
10
50
100
pCi/day
0.005
0.02
0.1
0.2
1.0
1
10
100
1000
Time after Inhalation (days)

FIGURE 4-8

Prediction of the simulation model, as modified for use with human data, for daily urinary excretion for Case 2

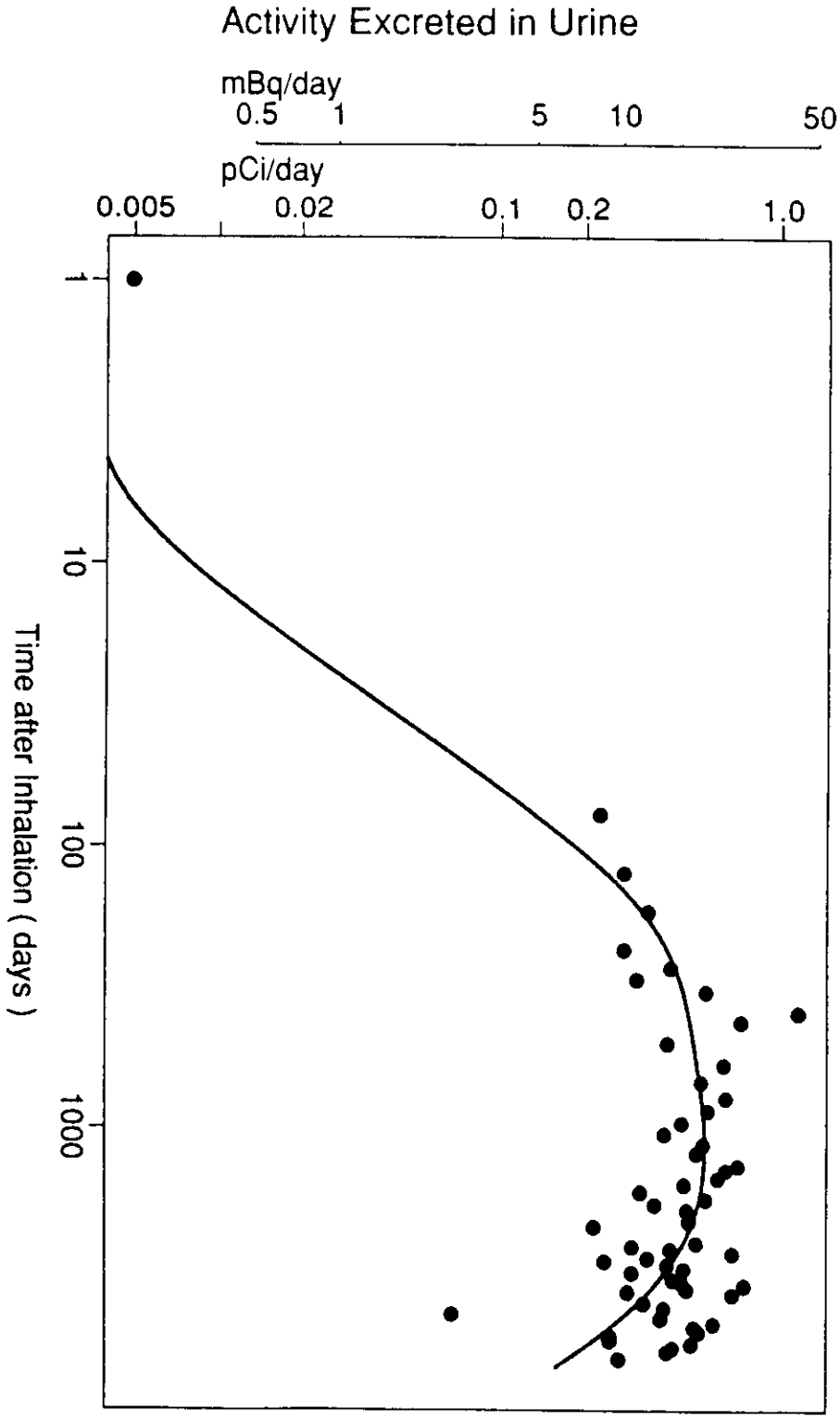
Activity Excreted in Urine
mBq/day
0.5
1
5
10
50
pCi/day
0.005
0.02
0.1
0.2
1.0
1
10
100
1000
Time after Inhalation (days)

FIGURE 4-9

Prediction of the simulation model, as modified for use with human data, for daily urinary excretion for Case 3

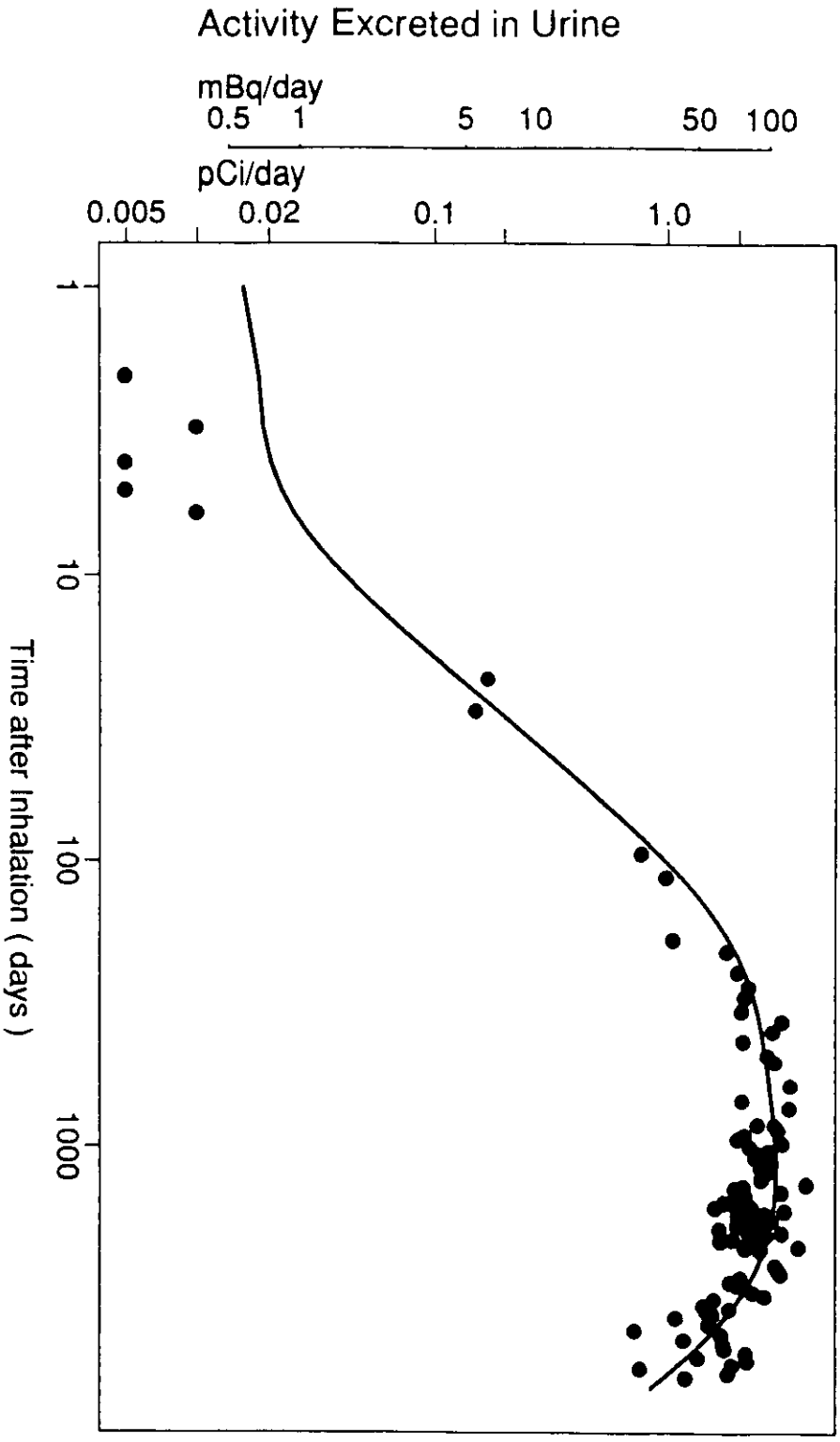
Activity Excreted in Urine
mBq/day
0.5
1
5
10
50
100
pCi/day
0.005
0.02
0.1
1.0
1
10
100
1000
Time after Inhalation (days)

FIGURE 4-10

Prediction of the simulation model, as modified for use with human data, for daily urinary excretion for Case 4

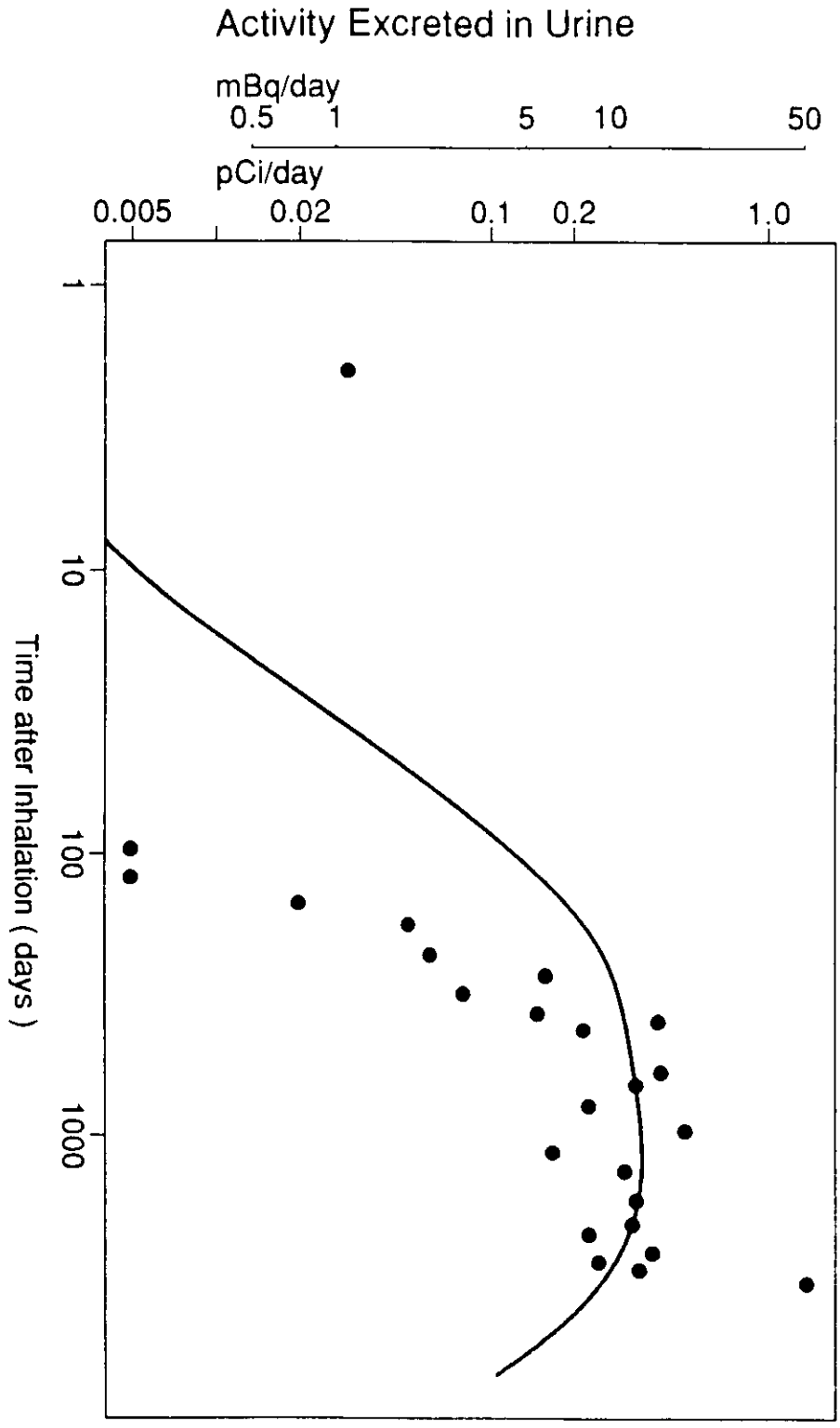
Activity Excreted in Urine
mBq/day
0.5
1
5
10
50
pCi/day
0.005
0.02
0.1
0.2
1.0
1
10
100
1000
Time after Inhalation (days)

FIGURE 4-11

Prediction of the simulation model, as modified for use with human data, for daily urinary excretion for Case 5

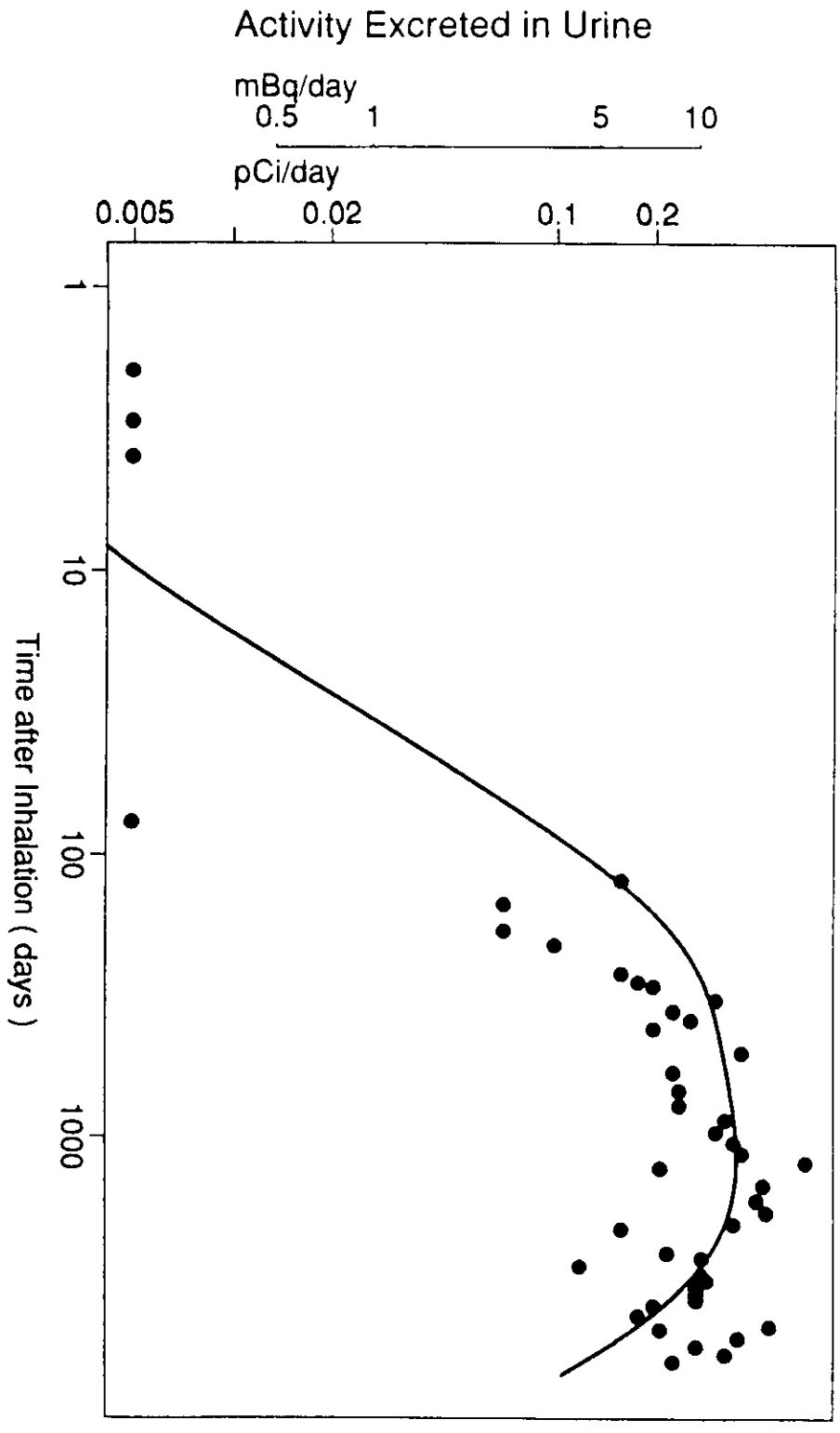
Activity Excreted in Urine
mBq/day
0.5
1
5
10
pCi/day
0.005
0.02
0.1
0.2
1
10
100
1000
Time after Inhalation (days)

FIGURE 4-12

Prediction of the simulation model, as modified for use with human data, for daily urinary excretion for Case 6

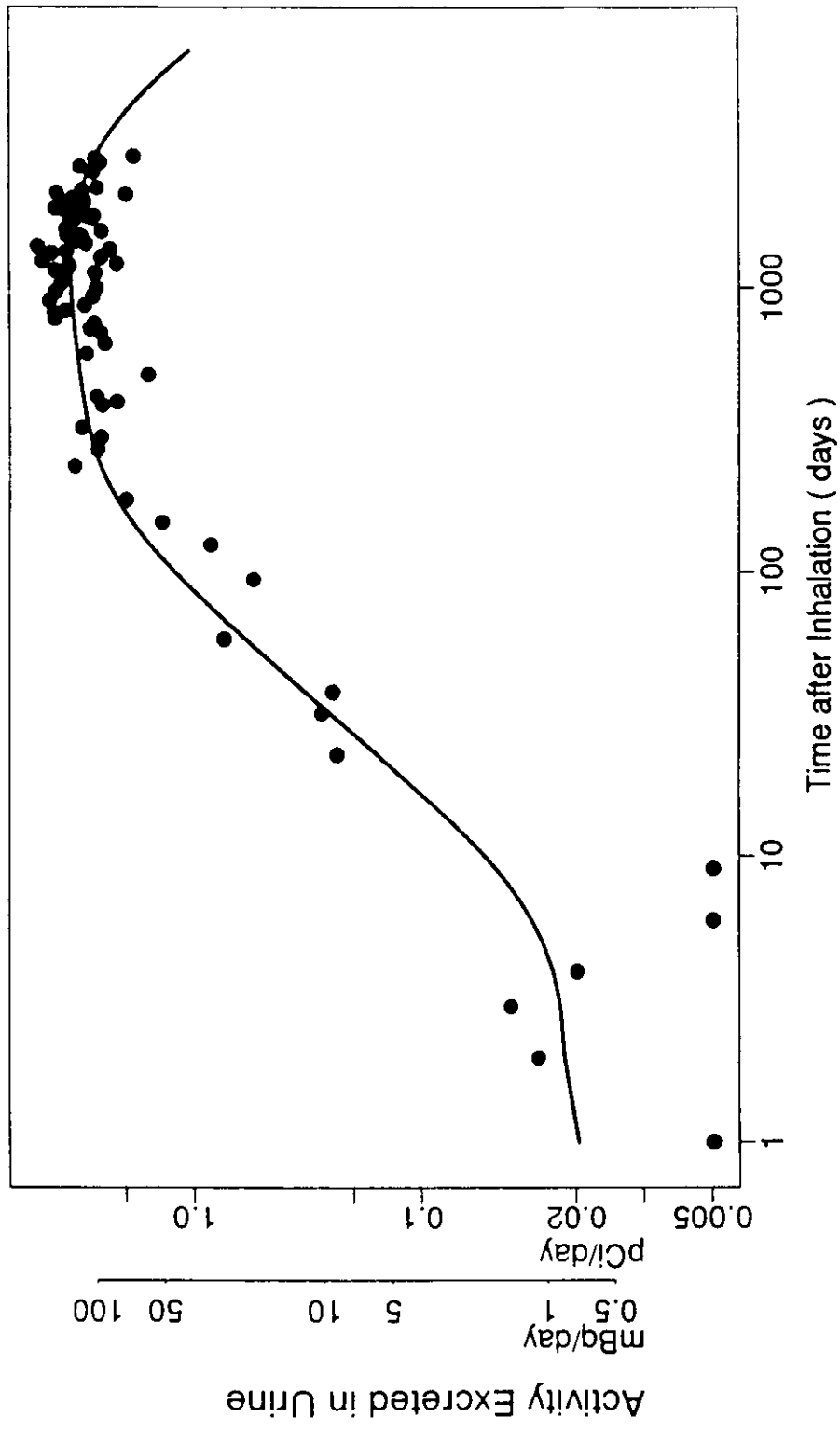
Activity Excreted in Urine
mBq/day
0.5
1
5
10
50
100
pCi/day
0.005
0.02
0.1
1.0
1
10
100
1000
Time after Inhalation (days)

FIGURE 4-13

Prediction of the simulation model, as modified for use with human data, for daily urinary excretion for Case 7

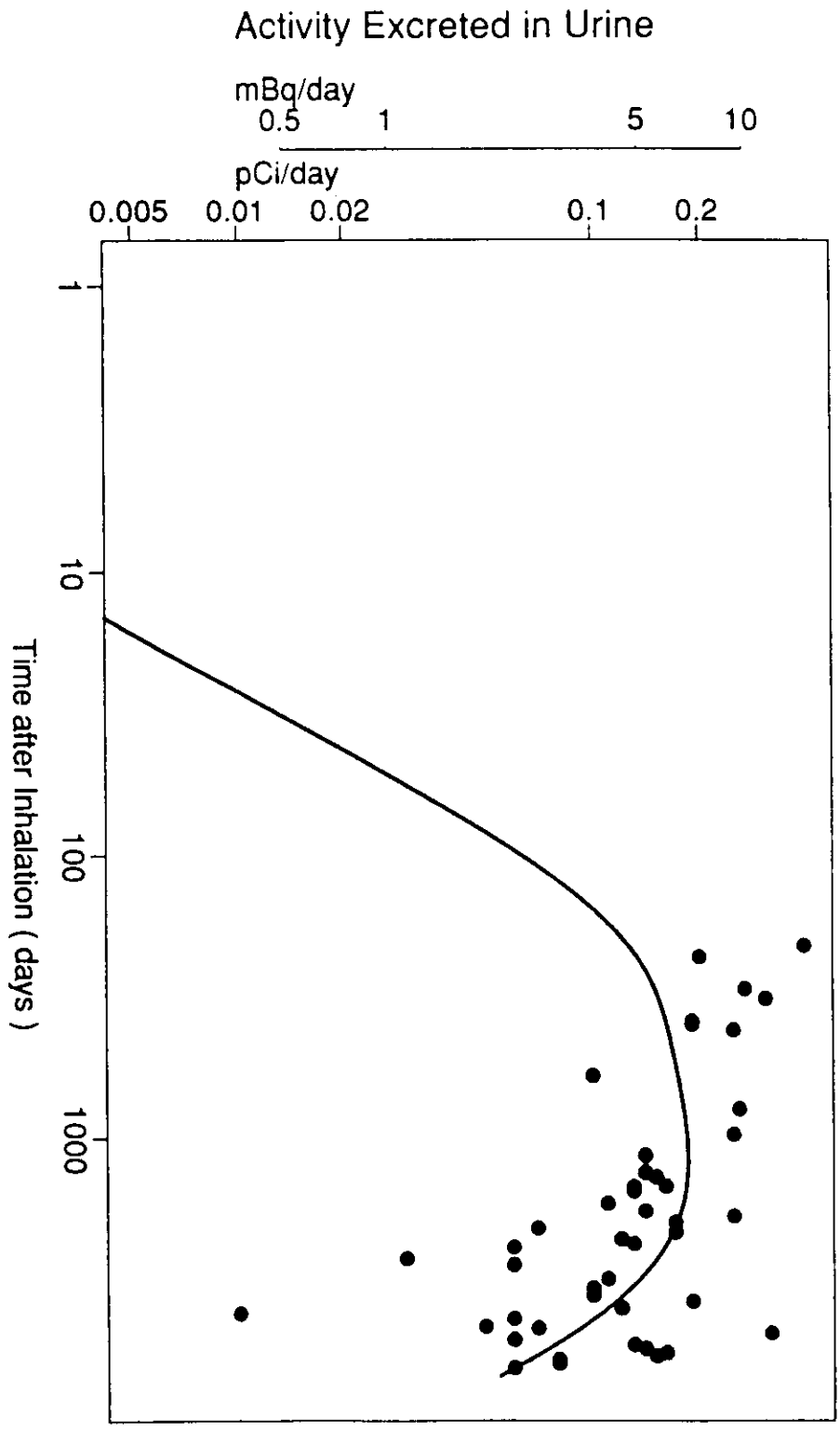
Activity Excreted in Urine
mBq/day
0.5
1
5
10
pCi/day
0.005
0.01
0.02
0.1
0.2
1
10
100
1000
Time after Inhalation (days)

TABLE 4-3

Estimated Initial Lung Burdens for the Seven Exposed Individuals in this Study

Exposed Individual	Estimated Initial Lung Burden nCi	Bq
Case 1	45	1700
Case 2	13	480
Case 3	70	2600
Case 4	8.7	320
Case 5	8.7	320
Case 6	87	3200
Case 7	4.5	170

Table 4-3 contains estimated initial lung burdens for the seven workers, which ranged from 4.5 to 87 nCi (170 to 3200 Bq). Most of the human data can be contained within excretion curves produced using ILBs a factor of two greater than and less than these estimates (e.g., most of the data for Case 1 falls in an envelope bounded by the excretion curves generated using ILBs of 22 and 90 nCi (650 and 3400 Bq)). Kathren and McInroy (1991), in their comparison of Pu deposition estimates from various models to autopsy data, found that the best estimates were within a factor of two for each of the cases examined. Because the predictive ability of biokinetic models is quite sensitive to the accuracy of the urinary excretion data and to accurate knowledge of the specific time and relative magnitude of exposure, they felt that agreement of model predictions with postmortem data within a factor of two to three "should probably be considered excellent" (p. 487).

At present, no autopsy data are available for comparison with the model predictions and use in validating them. However, one of the seven exposed individuals from this study is now deceased and was a whole-body donor to the United States Transuranium Registry. Analysis of autopsy results concerning retention and distribution of ^{238}Pu in the whole body is now in progress. These results, when available, can be compared to the model predictions. Preliminary analyses suggest that the estimates produced by the human model used in this study compare favorably to autopsy results (personal communication, J.F. McInroy to R.A. Guilmette).

To test the model's applicability to data other than that for which it was formulated, the model prediction for an injection exposure to ^{239}Pu was compared to excretion data from the studies by Langham et al. (1950) and Leggett and Eckerman (1987). Agreement between the model prediction and the data is generally good for the urinary excretion data from both studies; although the model underpredicts excretion at times less than about 7 d post-exposure and greater than 7000 d post-exposure, and overpredicts for times in between, the prediction is off by only about a factor of two. However, predicted fecal excretion does not match the pattern seen by Langham et al.

Conclusions

Modification of many of the aerosol characteristics and most of the rate constants used in the canine model was necessary for adapting it for use with human bioassay data. It was noted that the fragmentation rate parameter f seems to be the controlling factor in determining fragmentation rate. It was further noted that although changing several aerosol characteristics affected the peak level of activity excreted in urine and the time at which the peak occurred, only the particle solubility seemed to influence initial excretion levels. Although this would seem to imply that the increased surface area of fragments relative to particles does not influence excretion levels until some time has lapsed following inhalation, introducing a time delay into the expression for the fragmentation rate constant had no discernible effect on the shape of the excretion curve. Changes to the systemic rate constants produced retention half-times in the organs and partitioning among the organs that agree with those published in the literature.

Application of the modified model to urinary excretion data from seven individuals occupationally exposed to $^{238}PuO_2$ produced estimates of initial lung burden of 4.5 to 87 nCi (170 to 3200 Bq). Most of the excretion data could be contained in an envelope bounded by the excretion curves generated using ILBs a factor of two greater than and less than those estimated for the individuals. Although the

development of the excretion curve shape was weighted more heavily toward the more complete data sets, the curve provided a reasonable fit to all data sets. However, the urinary excretion patterns observed for the seven exposed humans are not identical, with cases 4 and 7 deviating most noticeably from the generalized pattern. These observed differences indicate that the biological factors driving urinary excretion, at least for these cases, are not completely understood.

Simulation of an injection exposure to ^{239}Pu provided good agreement between predicted and observed urinary excretion patterns; however, the fecal excretion curve fits were unsatisfactory. This is due at least in part to a lack of fecal excretion data for the subjects of this study. Thus, the canine model as modified for use with human data appears to give reasonable and useful results for application following both inhalation exposures to $^{238}PuO_2$, for which it was designed, and exposures to other isotopes and/or by other routes.

Recommendations for Future Work

Acquisition of more bioassay data from humans occupationally exposed to ^{238}Pu will allow the model validation process to be extended. Collection of urine samples from the six surviving cases from this study is ongoing, and these will add to our knowledge of late excretion. Of potentially

greater usefulness would be data from another exposure incident, especially fecal data and specific data on the aerosol characteristics, to provide an independent check on the current model.

In this study, the behavior of inhaled Pu in the human lungs was assumed to be similar to that seen in canine lungs. However, more research is needed on the fate of Pu in human lungs, especially on its binding to lung tissue and its retention in the lungs. The transformed compartment in the pulmonary and tracheobronchial lymph node (TBLN) regions, identified in animal studies, may not be directly applicable to humans. Similarly, although the TBLN region is useful in the canine model, further investigation is needed of the role the lymph nodes play in the retention and translocation of inhaled Pu in humans.

Although the fecal excretion pattern predicted by the human model were unsatisfactory, based on that seen in a previous study, the lack of fecal excretion data from the subjects of this study hampered efforts to modify fecal excretion parameters. As mentioned previously, obtaining fecal excretion data would aid in this effort. In addition, a better understanding of the biology of late fecal excretion (excretion of material cleared from the respiratory tract by other than mechanical clearance) would improve the modeling process. Appropriately designed animal studies could aid in understanding the metabolism of ^{238}Pu that is transferred to

the liver, as well as elucidating the importance of other potential excretion pathways such as movement of Pu from blood across the gut wall to feces.

Finally, model predictions of biological half-times in the liver for Pu may indicate an isotope effect, with ^{239}Pu being retained about twice as long as ^{238}Pu. Improved modeling of the liver, further investigation of human autopsy results, and appropriately designed animal studies could be used to determine the validity of this prediction.

APPENDIX

FINAL SIMULATION CODE USED FOR HUMAN DATA

PROGRAM - ACSL PROGRAM FOR BIOKINETIC MODELING OF Pu-238
(FILE:PU238NEW)

```
INITIAL

    CONSTANT  TC     =   2.16E-5,   ...
              K15A   =  20.,        ...
              K25A   =  20.,        ...
              K3A4A  =   2.E-3,     ...
              K3B4B  =   4.E-3,     ...
              K3CD   =  10.,        ...
              K3C6   =  90.,        ...
              K3D2   =   2.E-3,     ...
              K3D6   =   1.E-4,     ...
              K4CD   =  10.,        ...
              K4C6   =  90.,        ...
              K4D6   =   2.E-3,     ...
              K5AB   =  15.,        ...
              K5BC   =   5.0,       ...
              K5B6   =   1.E-3,     ...
              K65B   =   0.,        ...
              K5CF   =   4.,        ...
              K67A   =   0.6,       ...
              K7A6   =   1.9E-3,    ...
              K7AB   =   1.9E-4,    ...
              K7BA   =   7.6E-5,    ...
              K7A5B  =   9.4E-5,    ...
              K7B5B  =   4.7E-5,    ...
              K68A   =   0.6,       ...
              K8A6   =   1.9E-3,    ...
              K8AB   =   1.9E-4,    ...
              K8BA   =   5.4E-5,    ...
              K69A   =   1.0,       ...
              K9A6   =   0.05,      ...
              K9AB   =   5.E-3,     ...
              K9BA   =   1.9E-3,    ...
              K610A  =   5.E-3,     ...
              K10A6  =   1.9E-3,    ...
              K10AB  =   0.03,      ...
              K10BA  =   6.E-3,     ...
              K6U    =   0.06,      ...
```

```
            K10AU  =   0.,        ...
            BLOOD  =   1.0,       ...
            S      =   2.E+2,     ...
            ALS    =   6.0,       ...
            ALV    =   1.0,       ...
            XK     =   3.E-10,    ...
            DEN    =   8.0,       ...
            XMMD   =   4.8E-5,    ...
            SIGG   =   1.1,       ...
            EKM1   =   0.03,      ...
            GAM    =   0.3,       ...
            EKM2   =   8.E-4,     ...
            COEF   =   1.E-3,     ...
            A      =   0.48,      ...
            TDELAY =   0.

CONSTANT    A1IC   =   0.,        ...
            A2IC   =   0.,        ...
            A3AIC  =   1.,        ...
            A3BIC  =   0.,        ...
            A3CIC  =   0.,        ...
            A3DIC  =   0.,        ...
            A4AIC  =   0.,        ...
            A4BIC  =   0.,        ...
            A4CIC  =   0.,        ...
            A4DIC  =   0.,        ...
            A5AIC  =   0.,        ...
            A5BIC  =   0.,        ...
            ASIIC  =   0.,        ...
            A5CIC  =   0.,        ...
            A6IC   =   0.,        ...
            AABSIC =   0.,        ...
            A7AIC  =   0.,        ...
            A7BIC  =   0.,        ...
            ALIVIC =   0.,        ...
            A8AIC  =   0.,        ...
            A8BIC  =   0.,        ...
            ASKLIC =   0.,        ...
            A9AIC  =   0.,        ...
            A9BIC  =   0.,        ...
            A10AIC =   0.,        ...
            A10BIC =   0.,        ...
            AFIC   =   0.,        ...
            AUIC   =   0.,        ...
            A11IC  =   0.,        ...
            A12IC  =   0.,        ...
            ILB1   =   4.5E4,     ...
            ILB2   =   1.33E4,    ...
            ILB3   =   7.0E4,     ...
            ILB4   =   8.7E3,     ...
            ILB5   =   8.7E3,     ...
            ILB6   =   8.7E4,     ...
```

```
            ILB7    =    4.5E3


    VARIABLE  T       =    0.0   $ 'RENAME INDEPENDENT VARIABLE'
    ALGORITHM IALG    =    2     $ 'GEAR STIFF INTEGRATION'

    CONSTANT  TSTOP   =    2.E4  $ 'LENGTH OF EXPERIMENT'
    CONSTANT  POINTS  =    2.E3  $ 'NUMBER OF OUTPUT POINTS'

    CINT  =   TSTOP/POINTS       $    'SPECIFY    COMMUNICATION
                                 $  INTERVAL'


END

DYNAMIC

    DERIVATIVE

        A1     = INTEG(DA1,A1IC)
                 KD = FUND(T,ALS,ALV,XK,DEN,XMMD,SIGG)
                 DA1 = -(K15A+KD)*A1-TC*A1
        A2     = INTEG(DA2,A2IC)
                 KM = FUNM(T,EKM1,GAM,EKM2)
                 DA2 = KM*(A3A+A3B)+K3D2*A3D-(K25A+KD)*A2-TC*A2
        A3A    = INTEG(DA3A,A3AIC)
                 KF = FUNF(T,TDELAY,COEF,A)
                 DA3A = -(KF+KM+KD+K3A4A)*A3A-TC*A3A
        A3B    = INTEG(DA3B,A3BIC)
                 DA3B = KF*A3A-(KM+KD*S+K3B4B)*A3B-TC*A3B
        A3C    = INTEG(DA3C,A3CIC)
                 DA3C = KD*A3A+KD*S*A3B-(K3CD+K3C6)*A3C-TC*A3C
        A3D    = INTEG(DA3D,A3DIC)
                 DA3D = K3CD*A3C-(K3D2+K3D6)*A3D-TC*A3D
        A4A    = INTEG(DA4A,A4AIC)
                 DA4A = K3A4A*A3A-(KF+KD)*A4A-TC*A4A
        A4B    = INTEG(DA4B,A4BIC)
                 DA4B = K3B4B*A3B+KF*A4A-KD*S*A4B-TC*A4B
        A4C    = INTEG(DA4C,A4CIC)
                 DA4C = KD*A4A+KD*S*A4B-(K4CD+K4C6)*A4C-TC*A4C
        A4D    = INTEG(DA4D,A4DIC)
                 DA4D = K4CD*A4C-K4D6*A4D-TC*A4D
        A5A    = INTEG(DA5A,A5AIC)
                 DA5A = K15A*A1+K25A*A2-K5AB*A5A-TC*A5A
        A5B    = INTEG(DA5B,A5BIC)
                 DA5B = K5AB*A5A+BLOOD*K65B*A6+...
                        K7A5B*A7A+K7B5B*A7B-...
                        (K5BC+K5B6)*A5B-TC*A5B
        DASI   = K5AB*A5A+K7A5B*A7A+K7B5B*A7B
        A5C    = INTEG(DA5C,A5CIC)
                 DA5C = K5BC*A5B-K5CF*A5C-TC*A5C
```

```
      DALI   = K5BC*A5B
      A6     = INTEG(DA6,A6IC)
               DA6 = KD*(A1+A2)+K3C6*A3C+K3D6*A3D+...
                     K4C6*A4C+K4D6*A4D+K5B6*A5B+...
                     K7A6*A7A+K8A6*A8A+...
                     K9A6*A9A+K10A6*A10A-...
                    BLOOD*(K65B+K67A+K68A+K69A+K610A)*A6-...
                     K6U*A6-TC*A6
      AABS   = INTEG(DAABS,AABSIC)
               DAABS = KD*(A1+A2)+K3C6*A3C+K3D6*A3D+...
                       K4C6*A4C+K4D6*A4D
      A7A    = INTEG(DA7A,A7AIC)
               DA7A = BLOOD*K67A*A6+K7BA*A7B-...
                      (K7A5B+K7A6+K7AB)*A7A-TC*A7A
      A7B    = INTEG(DA7B,A7BIC)
               DA7B = K7AB*A7A-(K7BA+K7B5B)*A7B-TC*A7B
      ALIV   = INTEG(DALIV,ALIVIC)
               DALIV = BLOOD*K67A*A6+K7BA*A7B
      DABILE= K7A5B*A7A+K7B5B*A7B
      A8A    = INTEG(DA8A,A8AIC)
               DA8A = BLOOD*K68A*A6+K8BA*A8B-...
                      (K8A6+K8AB)*A8A-TC*A8A
      A8B    = INTEG(DA8B,A8BIC)
               DA8B = K8AB*A8A-K8BA*A8B-TC*A8B
      ASKL   = INTEG(DASKL,ASKLIC)
               DASKL = BLOOD*K68A*A6+K8BA*A8B
      A9A    = INTEG(DA9A,A9AIC)
               DA9A = BLOOD*K69A*A6+K9BA*A9B-...
                      (K9A6+K9AB)*A9A-TC*A9A
      A9B    = INTEG(DA9B,A9BIC)
               DA9B = K9AB*A9A-K9BA*A9B-TC*A9B
      A10A   = INTEG(DA10A,A10AIC)
               DA10A = BLOOD*K610A*A6+K10BA*A10B-...
                       (K10AB+K10BA+K10AU)*A10A-TC*A10A
      A10B   = INTEG(DA10B,A10BIC)
               DA10B = K10AB*A10A-K10BA*A10B-TC*A10B
      AF     = INTEG(DAF,AFIC)
               DAF = K5CF*A5C-TC*AF
      AU     = INTEG(DAU,AUIC)
               DAU = K6U*A6+K10AU*A10A-TC*AU
      A11    = INTEG(DA11,A11IC)
               DA11 = K5CF*A5C
      A12    = INTEG(DA12,A12IC)
               DA12 = K6U*A6+K10AU*A10A
      U1     = DA12*ILB1
      U2     = DA12*ILB2
      U3     = DA12*ILB3
      U4     = DA12*ILB4
      U5     = DA12*ILB5
      U6     = DA12*ILB6
      U7     = DA12*ILB7
END
```

```
      IF (A6.GT.0.) UBR=DA12/A6
      IF (DA12.GT.0.) BUR=A6/DA12
      IF (DA11.GT.0.) UFR=DA12/DA11
      IF (DA12.GT.0.) FUR=DA11/DA12
      IF (A11.GT.0.) TUF=A12/A11
      IF (A12.GT.0.) TFU=A11/A12
      IF (DABILE.GT.0.) UBIR=DA12/DABILE
      IF (DA12.GT.0.) BIUR=DABILE/DA12
      IF (DASI.GT.0.) USIR=DA12/DASI
      IF (DA12.GT.0.) SIUR=DASI/DA12
      IF (DALI.GT.0.) ULIR=DA12/DALI
      IF (DA12.GT.0.) LIUR=DALI/DA12

      IF (T.LT.10.) CINT=1.
      IF (T.GE.10.) CINT=10.

      A3     = A3A+A3B+A3C+A3D
      A4     = A4A+A4B+A4C+A4D
      A5     = A5A+A5B+A5C
      A7     = A7A+A7B
      A8     = A8A+A8B
      A9     = A9A+A9B
      A10    = A10A+A10B
      ALUNG  = A2+A3

      LEFTM  = (A3AIC+A6IC)*EXP(-TC*T)
      MATBAL= (LEFTM-A1-A2-A3-A4-A5-A6-A7-A8-A9-A10-AF-AU)/LEFTM

      BFRAC  = (A1+A2+A3+A4+A5+A6+A7+A8+A9+A10)/(A3AIC+A6IC)
      BBURD1= ILB1*BFRAC
      BBURD2= ILB2*BFRAC
      BBURD3= ILB3*BFRAC
      BBURD4= ILB4*BFRAC
      BBURD5= ILB5*BFRAC
      BBURD6= ILB6*BFRAC
      BBURD7= ILB7*BFRAC

      TERMT(T.GE.TSTOP)          $'DEFINE TERMINATION CONDITION'

END

TERMINAL

      END

END

          REAL FUNCTION FUND(T,ALS,ALV,XK,DEN,XMMD,SIGG)
          IMPLICIT REAL*8(A-H,O-Z), INTEGER(I-N)
          REAL*4 T,F
          DIMENSION U(4), QF(4)
C
```

```
C****    CALCULATED CONSTANTS  ********************************
C
         C    = ALS*XK/ALV/DEN/XMMD
         PI   = 3.14159
         C2P = 1/DSQRT(2*PI)
         SIG = DLOG(SIGG)
C
C****    CALCULATE DERIVATIVE OF XF NUMERICALLY   ************
C
         IF (T .EQ. 0.) THEN
             T = 1.E-30
         END IF
         DO 10 I=1,4
             U(I) = C1+SIG(I-1)
             PF = DNORDF(U(I))
             QF(I) = 1-PF
    10   CONTINUE
C
         A1 = -C1**2/2.
         IF (A1 .LE. -80.) THEN
             A1 = -80.
             A2 = -80.
             A3 = -80.
             A4 = -80.
         ELSE
             A2 = 0.5*SIG**2-(C1+SIG)**2/2
             A3 = 2*SIG**2-(C1+2*SIG)**2/2
             A4 = 4.5*SIG**2-(C1+3*SIG)**2/2
         END IF
C
         DF = C2P*(-DEXP(A1)/SIG/T+
        1      C/SIG*DEXP(A2)-
        1      C**2*T/3/SIG*DEXP(A3)+
        1      C**3*T**2/27/SIG*DEXP(A4))+
        1      (-C*DEXP(0.5*SIG**2)*QF(2)+
        1      C**2*T*2/3*DEXP(2*SIG**S)*QF(3)-
        1      C**3*T**2/9*DEXP(4.5*SIG**2)*QF(4))
C
C****    CALCULATE XF AT TIME=T   *****************************
C
         XF1 = QF(1)-C*T*DEXP(0.5*SIG**2)*QF(2)+
        1       C**2*T**2/3*DEXP(2*SIG**2)*QF(3)-
        1       C**3*T**3/27*DEXP(4.5*SIG**2)*QF(4)
C
         FUND = SNGL(-DF/XF1)
         RETURN
         END

         REAL FUNCTION FUNM(T,EKM1,GAM,EKM2)
C
         FUNM = SNGL(EKM1*EXP(-GAM*T)+EKM2)
         RETURN
```

```
      END

      REAL FUNCTION FUNF(T,TDELAY,COEF,A)
C
      IF (T .LT. TDELAY) TFRAG=0.
      IF (T .GE. TDELAY) TFRAG=T-TDELAY

      FUNF = SNGL(COEF*TFRAG**A)
      RETURN
      END
```

REFERENCES

Beach, S.A., and Dolphin, G.W., "Determination of Plutonium Body Burdens from Measurements of Daily Urine Excretion," in Assessment of Radioactivity in Man, Vol. 2, pp. 603-615, International Atomic Energy Agency, Vienna, Austria (1964).

Boecker, B., Hall, R., Inn, K., Lawrence, J., Ziemer, P., Eisele, G., Wachholz, B., and Burr, W., "Current Status of Bioassay Procedures to Detect and Quantify Previous Exposures to Radioactive Materials," Health Physics 60, Supplement 1, 45-100 (1991).

Bustad, L.K., Stitzel, K.A., Haro, E.K., and Goldman, M., "The Choice of the Beagle for Radiobiologic Studies," in Radiobiology of Plutonium (edited by B.J. Stover and W.S.S. Jee), pp. 203-211, The J.W. Press, Salt Lake City, Utah (1972).

Diel, J.H., and Mewhinney, J.A., "Toxicity of Inhaled $^{238}PuO_2$ I. Metabolism," in Proceedings of the Fifth International Congress of IRPA, Jerusalem, Israel, Vol. II, pp. 107-110 (1980).

Diel, J.H., and Mewhinney, J.A., "Fragmentation of Inhaled $^{238}PuO_2$ Particles in Lung," Health Physics 44, 135-145 (1983).

Durbin, P.W., "Plutonium in Man: A New Look at the Old Data," in Radiobiology of Plutonium (edited by B.J. Stover and W.S.S. Jee), pp. 469-530, The J.W. Press, Salt Lake City, Utah (1972).

Durbin, P.W., and Jeung, N., "Reassessment of Distribution of Plutonium in the Human Body Based on Experiments with Non-Human Primates," in The Health Effects of Plutonium and Radium (edited by W.S.S. Jee), pp. 297-313, The J.W. Press, Salt Lake City, Utah (1976).

Fleischer, R.L., and Raabe, O.G., "Fragmentation of Respirable PuO_2 Particles in Water by Alpha Decay--A Mode of 'Dissolution,'" Health Physics 32, 253-257 (1977).

Goldman, M., Rosenblatt, L.S., and Book, S.A., "Lifetime Radiation Effects Research in Animals: An Overview of the Status and Philosophy of Studies at (the) University of California-Davis Laboratory for Energy-Related Health Research," in Life-Span Radiation Effects Studies in Animals: What Can They Tell Us? (edited by R.C. Thompson and J.A. Mahaffy), pp. 53-65, Office of Scientific and Technical Information, U.S. Department of Energy, Washington, D.C. (1986).

Guilmette, R.A., and Mewhinney, J.A., "A Biokinetic Model of Inhaled Cm Compounds in Dogs: Application to Human Data," Health Physics 57, Supplement 1, 187-198 (1989).

International Commission on Radiological Protection, Limits on Intakes of Radionuclides by Workers, ICRP Publication 30, Part I, Pergamon Press, Oxford, England (1979).

International Commission on Radiological Protection, The Metabolism of Plutonium and Related Elements, ICRP Publication 48, Pergamon Press, Oxford, England (1986).

International Commission on Radiological Protection, Individual Monitoring for Intakes of Radionuclides by Workers: Design and Interpretation, ICRP Publication 54, Pergamon Press, Oxford, England (1987).

Kathren, R.L., and McInroy, J.F., "Comparison of Systemic Plutonium Deposition Estimates from Urinalysis and Autopsy Data in Five Whole-Body Donors," Health Physics 60, 481-488 (1991).

Kathren, R.L., McInroy, J.F., Reichert, M.M., and Swint, M.J., "Partitioning of ^{238}Pu, ^{239}Pu and ^{241}Am in Skeleton and Liver of U.S. Transuranium Autopsy Cases," Health Physics 54, 181-188 (1988).

Langham, W.H., Bassett, S.H., Harris, P.S., and Carter, R.E., Distribution and Excretion of Plutonium Administered to Man, LA-1151, Los Alamos Scientific Laboratory, Los Alamos, New Mexico (1950) See Health Physics 38, 1031-1060 (1980).

Leggett, R.W., "A Model of the Retention, Translocation, and Excretion of Systemic Pu," Health Physics 49, 1115-1137 (1985).

Leggett, R.W., and Eckerman, K.F., "A Method for Estimating the Systemic Burden of Pu from Urinalysis," Health Physics 53, 337-346 (1987).

McInroy, J.F., Kathren, R.L., and Swint, M.J., "Distribution of Plutonium and Americium in Whole Bodies Donated to the United States Transuranium Registry," Radiation Protection Dosimetry 26, 151-158 (1989).

McInroy, J.F., Kathren, R.L., Voelz, G.L., and Swint, M.J., "U.S. Transuranium Registry Report on the ^{239}Pu Distribution in a Human Body," Health Physics 60, 307-333 (1991).

Mercer, T.T., "On the Role of Particle Size in the Dissolution of Lung Burdens," Health Physics 13, 1211-1221 (1967).

Mewhinney, J.A., and Diel, J.H., "Retention of Inhaled $^{238}PuO_2$ in Beagles: A Mechanistic Approach," Health Physics 45, 39-60 (1983).

Muggenburg, B.A., Mewhinney, J.A., Merickel, B.S., Boecker, B.B., Hahn, F.F., Guilmette, R.A., Mauderly, J.L., and McClellan, R.O., "Toxicity of Inhaled $^{238}PuO_2$ II. Biological Effects in Beagle Dogs," in Proceedings of the Fifth International Congress of IRPA, Jerusalem, Israel, Vol. II, pp. 115-118 (1980).

National Council on Radiation Protection and Measurements, Use of Bioassay Procedures for Assessment of Internal Radionuclide Deposition, NCRP Report No. 87, Bethesda, Maryland (1987).

Park, J.F., Case, A.C., and Catt, D.L., "Dose-Effect Studies with Inhaled Plutonium Oxide in Dogs," in Pacific Northwest Laboratory Annual Report for 1979, Part I. Biomedical Sciences, PNL-3300, Richland, Washington, pp. 87-94 (1980).

Stannard, J.N., "Biomedical Aspects of Plutonium (Discovery, Development, Projections)," in Uranium, Plutonium, Transplutonic Elements (edited by H.C. Hodge, J.N. Stannard, and J.B. Hursh), pp. 309-322, Springer Verlag, New York (1973).

Stannard, J.N., "Radiation Protection and the Internal Emitter Saga," in Health and Ecological Implications of Radioactively Contaminated Environments: Proceedings of the Twenty-sixth Annual Meeting of the National Council on Radiation Protection and Measurements, pp.157-189, NCRP, Bethesda, Maryland (1990).

Stover, B.J., Atherton, D.R., and Keller, N., "Metabolism of ^{239}Pu in Adult Beagle Dogs," Radiation Research 10, 130-147 (1959).

Stradling, G.N., Ham, G.J., Smith, H., Cooper, J., and Breadmore, S.E., "Factors affecting the mobility of plutonium-238 dioxide in the rat," International Journal of Radiation Biology 34, 37-47 (1978).

Task Group on Lung Dynamics, "Deposition and Retention Model for Internal Dosimetry of the Human Respiratory Tract," Health Physics 12, 173-207 (1966).

Turcotte, R.P., "Structural Changes in Actinide Dioxides Under Self- and Reactor Irradiation," in Plutonium and Other Actinides (edited by H. Black and R. Linder), pp. 851-859, North-Holland Publishing Company, Amsterdam (1976).

United States Department of Energy Office of Special Applications, Final Safety Analysis Report for the Ulysses Mission. Volume III (Book 2) Nuclear Risk Analysis Document--Appendices, ULS-FSAR-006, Washington, D.C. (1990).

United States Nuclear Regulatory Commission, Interpretation of Bioassay Measurements, NUREG/CR-4884, Washington, D.C. (1987).

Walker, W.F., Parrington, J.R., and Feiner, F., Nuclides and Isotopes: Fourteenth Edition, General Electric Company, San Jose, California (1989).

BIOGRAPHICAL SKETCH

Albert Wayne Hickman, Jr., [redacted] When Bert was nine, he moved across Pensacola Bay with his family to Gulf Breeze, where he graduated from Gulf Breeze High School in 1982. During his high school years, Bert was a member of the marching, concert, and jazz bands. He also participated in the youth activities at the First Baptist Church of Pensacola. In addition to membership in the National Honor Society (which he served as president), French Honor Society (which he served as secretary-treasurer), and Mu Alpha Theta math honor society, during his senior year Bert was selected as one of 144 Presidential Scholars, an honor bestowed by the United States Department of Education.

In August 1982, Bert began his studies at the University of Florida, where he was both a National Merit Scholar and an Institute of Nuclear Power Operations scholar. While at Florida as an undergraduate, he participated in the lower division (freshman and sophomore) Honors Program and served as president of the affiliated Student Honors Organization. He also was elected to membership in Tau Beta Pi engineering honor society, was a member of the American Institute of Chemical Engineers and the university marching band, and was

actively involved at the First Baptist Church of Gainesville. He received the Bachelor of Science in Chemical Engineering (with honors) in May 1987.

From August 1987 to June 1989, Bert served as the youth director at North Sea Baptist Church, an English-language congregation in Stavanger, Norway, under the sponsorship of the Foreign Mission Board of the Southern Baptist Convention. Upon his return to the United States, he began his graduate work in health physics, supported by a U.S. Department of Energy Nuclear Engineering/Health Physics Fellowship. While at the university for graduate work, Bert has been elected to membership in Alpha Nu Sigma, the nuclear honor society, and currently serves as its secretary-treasurer. He is again an active member of the First Baptist Church, where he has been working with middle schoolers and has participated in many areas of the music ministry.

I certify that I have read this study and that in my opinion it conforms to acceptable standards of scholarly presentation and is fully adequate, in scope and quality, as a thesis for the degree of Master of Science.

Genevieve S. Roessler, Chair
Associate Professor of Nuclear
Engineering Sciences

I certify that I have read this study and that in my opinion it conforms to acceptable standards of scholarly presentation and is fully adequate, in scope and quality, as a thesis for the degree of Master of Science.

David E. Hintenlang
Assistant Professor of Nuclear
Engineering Sciences

I certify that I have read this study and that in my opinion it conforms to acceptable standards of scholarly presentation and is fully adequate, in scope and quality, as a thesis for the degree of Master of Science.

Raymond A. Guilmette
Scientist, Inhalation Toxicology
Research Institute
Albuquerque, New Mexico

This thesis was submitted to the Graduate Faculty of the College of Engineering and to the Graduate School and was accepted as partial fulfillment of the requirements for the degree of Master of Science.

August 1991

Winfred M. Phillips
Dean, College of Engineering

Madelyn M. Lockhart
Dean, Graduate School